Food Research International 175 (2024) 113654

Contents lists available at ScienceDirect

Food Research International

journal homepage: www.elsevier.com/locate/foodres

Comprehensive metabolite and biological profile of "Sulmona Red Garlic" ecotype's aerial bulbils

Annalisa Chiavaroli [a,1], Fabrizio Masciulli [b,c,1], Cinzia Ingallina [b,c], Luisa Mannina [b,c], Maria Loreta Libero [a], Simonetta Cristina Di Simone [a], Alessandra Acquaviva [a], Nilofar [a], Lucia Recinella [a], Sheila Leone [a], Luigi Brunetti [a], Simone Carradori [a], Luca Cantò [a], Giustino Orlando [a,*], Gokhan Zengin [d], Abdullah Ibrahim Uba [e], Ugur Cakilcioğlu [f], Muzaffer Mukemre [g], Omer Elkiran [h], Maura Di Vito [i], Luigi Menghini [a,*], Claudio Ferrante [a]

[a] Department of Pharmacy, G. d'Annunzio University of Chieti-Pescara, Chieti, Italy
[b] Food Chemistry Lab, Department of Chemistry and Technology of Drugs, Sapienza University of Rome, Piazzale Aldo Moro 5, 00185 Rome, Italy
[c] NMR Lab, Sapienza University of Rome, Piazzale Aldo Moro 5, 00185 Rome, Italy
[d] Physiology and Biochemistry Laboratory, Department of Biology, Science Faculty, Selcuk University, Konya, Turkey
[e] College of Science and Mathematics, Rowan University, Glassboro, NJ 08028, United States
[f] Pertek Sakine Genç Vocational School, Munzur University, Tunceli, Pertek 62500, Turkey
[g] Department of Plant and Animal Production, Yuksekova Vocational School, Hakkari University, Hakkari 30100, Turkey
[h] Vocational School of Health Services, Department of Environmental Health, Sinop University, Sinop, Turkey
[i] Dip. di Scienze biotecnologiche di base, cliniche intensivologiche e perioperatorie Università Cattolica del Sacro Cuore, Largo Agostino Gemelli, 00168 Rome, Italy

ARTICLE INFO

Keywords:
NMR-metabolomic profile
Organosulphur compounds
Phenolic compounds
Eco-toxicological assays
Colon cancer
TRPM8

ABSTRACT

"Sulmona Red Garlic" is a well-known Italian traditional product. Bulbs, used for culinary purposes, have been largely investigated for their medicinal properties whereas aerial bulbils are usually removed as waste material. Here, for the first time, chemical composition and biological properties of the hydroalcoholic extract from aerial bulbils were investigated. Complementary information on metabolite composition were obtained using both NMR based untargeted and HPLC-DAD targeted methodologies. The NMR analysis revealed the presence of sugars, organic acids, amino acids, organosulphur compounds (methiin, alliin, allicin and cycloalliin), and other secondary metabolites. In particular, methiin and alliin were identified for the first time in the NMR spectra of aerial bulbil garlic extracts. Polyphenol content was determined by HPLC-DAD analysis: catechin, chlorogenic acid, and gallic acid turned out to be the most abundant phenolics.

Hydroalcoholic extract blocked cell proliferation of colon cancer cell line HCT116 with an IC_{50} of 352.07 μg/mL, while it was non-toxic to myoblast cell line C2C12. In addition, it caused seedling germination reduction of two edible and herbaceous dicotyledon species, namely *Cichorium intybus* and *C. endivia*. Moreover, the same extract reduced the gene expression of TNF-α (tumor necrosis factor), HIF1-α (hypoxia-inducible factor), VEGFA (vascular endothelial growth factor), and transient receptor potential (TRP) M8 (TRPM8) indicating the ability to contrast cancer development through the angiogenic pathway. Final, *in silico* experiments were also carried out supporting the biological effects of organosulphur compounds, particularly alliin, which may directly interact with TRPM8.

The results here reported suggest the potential use of garlic aerial bulbils often considered a waste product as a source in phytotherapeutic remedies.

* Corresponding authors.
E-mail addresses: annalisa.chiavaroli@unich.it (A. Chiavaroli), maria.libero@unich.it (M. Loreta Libero), simonetta.disimone@unich.it (S.C. Di Simone), alessandra.acquaviva@unich.it (A. Acquaviva), nilofar.nilofar@unich.it (Nilofar), lucia.recinella@unich.it (L. Recinella), sheila.leone@unich.it (S. Leone), luigi.brunetti@unich.it (L. Brunetti), simone.carradori@unich.it (S. Carradori), luca_canto@yahoo.it (L. Cantò), giustino.orlando@unich.it (G. Orlando), gokhanzengin@selcuk.edu.tr (G. Zengin), maura.divito@unicatt.it (M. Di Vito), luigi.menghini@unich.it (L. Menghini).
[1] These authors equally contributed to the study.

https://doi.org/10.1016/j.foodres.2023.113654
Received 9 August 2023; Received in revised form 25 October 2023; Accepted 31 October 2023
Available online 2 November 2023

1. Introduction

Garlic (*Allium sativum* L.) a member of the Amaryllidaceae family, has been used worldwide for culinary and medicinal purposes since ancient times. Bulbs are the most commonly used part of the plant; leaves and flowers are also edible but their consumption is limited as they are rather considered waste products.

Garlic aerial flowers, known as bulbils, are small bulb-like structures that form above the ground on the flower stalks of garlic plants. These bulbils are reproductive structures that contain embryonic garlic plants and can develop when garlic plants are allowed to flower, as they are a mean of propagation for the plant. However, cultivated garlic is usually grown from seed cloves, and aerial bulbils are typically removed early on to prevent flowering and promote bulb growth (Kamenetsky et al., 2004). These aerial bulbils can be used as a local food resource or for biotechnology purposes, making them potentially interesting by-products (Dong et al., 2022; Kajimura et al., 2000; Mathew et al., 2005). Literature studies report generally the phytochemical profile and the biological properties of garlic bulbs and leaves (Kasprzak-Drozd et al., 2022; Masashi et al., 2020; Šnirc et al., 2023) whereas aerial bulbils have not yet been investigated.

Among the various garlic ecotypes, "Sulmona Red Garlic" is a well-known Italian traditional product listed in the "National Register of Horticultural Varieties" (DM 296/2009 delivered by the Italian Ministry of Agricultural, Food and Forestal Policy; "Sulmona Red Garlic", Ark of taste, Slow Food Foundation for Biodiversity). It has been grown for a long time in the Abruzzo region, specifically in the surroundings of Sulmona. Bulbs are characterized by a mottled wine-red tunic, whereas, according to the production regulation, the aerial bulbils are removed, being a waste material of this food chain. However, the careful and manual work underlying the selection of the bulbils in the productive chain makes this by-product a high-quality plant material that is also considered a second line-line commercial product (La Salvia et al., 2022). Previous pharmacological studies conducted on the bulbs of "Sulmoma red garlic" demonstrated antioxidant and anti-inflammatory effects in brain synaptosomes and monocytes, respectively (Brunetti et al., 2009; Lasalvia et al., 2022). The chemical profile of bulbs from Sulmona Red Garlic have been also investigated using different analytical techniques (Ritota et al.,2012; Ferioli et al., 2020; La Salvia et al., 2011; La Salvia et al.,2020; Biancolillo et al., 2020).

In these investigations, the organo-sulphur compounds and other metabolome components, such as amino acids, fatty acids, organic acids and sugars, were recognised as promising quality and traceability indicators to assess the garlic provenance or variety (Ritota et al., 2012; Biancolillo et al., 2020), to assess the efficiency of different extraction methods (Ferioli et al., 2020), and to correlate the chemical composition to the biological properties (La Salvia et. al, 2022) including cardioprotective (Recinella et al., 2021) and cholesterol-lowering effects (Liu et al., 2000), inhibiting carcinogenesis and cancer growth (Shirin et al., 2001; Yan et al., 2013), and enhancing immunocompetence (Xu et al., 2018, ; Nantz et al., 2012).

Recently, the interest in garlic's potential to protect against inflammatory bowel diseases (IBDs) has significantly grown. Polar extracts from Nubia ecotype bulbs have shown an effect in reducing the burden of inflammation and oxidative stress, in isolated mouse colon (Recinella et al., 2022). Studies on rats have shown that garlic oil, which contains beneficial organosulphur compounds like allicin, can help reduce tissue damage caused by inflammation in an experimental in vivo model of colitis (Tanrıkulu, Şen Tanrıkulu, Kılınç, Can, & Köktürk, 2020). Additionally, clinical studies have pointed to a reduction of colon adenomas through the modulation of natural killer cell activity (Ansary et al., 2020). These effects have been associated to the presence in bulbis of specialized metabolites, such as sulphur and phenolic compounds (Kopeć et al., 2020). Sulphur compounds have shown protective effects in the colon, in terms of both anti-inflammatory and chemopreventive effects (Saud et al., 2016; Vezza et al., 2019). Similarly, phenolic compounds have long been involved in inhibiting the production of inflammatory mediators, in isolated colon exposed to inflammatory stimulus (Ferrante et al., 2019; Menghini et al., 2016; Menghini et al., 2018; Recinella et al., 2022).

In the present study, for the first time, the hydroalcoholic extracts of aerial bulbils of "Sulmona Red Garlic" have been investigated to obtain the chemical composition and biological properties. The phytochemical composition has been obtained by applying both untargeted and targeted analytical methodologies. In particular, untargeted Nuclear Magnetic Resonance (NMR) was used to obtain a comprehensive metabolite profile, allowing the identification and quantification of many compounds at once (Mannina, Sobolev, & Capitani, 2012; Mannina, Sobolev, & Viel, 2012). Targeted HPLC-DAD was used to obtain the phenolic profile. Cytotoxic effects of the bulbil extract were studied in the human colon cancer (HCT116) cell line, in which the gene expression of transient receptor potential (TRP) M8 (TRPM8), possibly involved in colon carcinogenesis (Borrelli et al., 2014), was measured. Additionally, the gene expression of inflammatory and angiogenic mediators such as tumor necrosis factor (TNF)α, hypoxia-inducible factor (HIF)1α, and vascular endothelial growth factor (VEGF)A was evaluated. Finally, *in silico* experiments, including components-targets analysis and docking runs, were conducted for unravelling the putative mechanisms underlying the observed biological effects.

2. 2 Materials and Methods

2.1. Chemicals

Double-distilled water was obtained using a Millipore Milli-Q Plus water treatment system (Millipore Bedford Corp., Bedford, MA, USA). EDTA deuterated was purchased from Cambridge Isotope laboratories, Inc. (Andover, USA). Monobasic potassium phosphate (KH_2PO_4) and dibasic potassium phosphate (K_2HPO_4) were purchased from Sigma-Aldrich S.r.l. (Milan, Italy). Deuterated water (D_2O) 99.97 atom% of deuterium, methanol-d_4 99.80 atom% of deuterium. 3-(Trimethylsilyl)-propionic-2,2,3,3-d_4 acid sodium salt (TSP) was purchased from Merck (Milan, Italy).

2.2. Sampling and sample preparation to perform HPLC analysis and biological assays

Plant material was sampled during the transformation process, from a commercial batch produced by "Aglio D'Alessandro" company (Pratola Peligna, L'Aquila, Italy). The plant material was a kind gift from "Aglio D'Alessandro" company. According to the "Sulmona Red Garlic" production regulation ("Sulmona Red Garlic", Ark of taste, Slow Food Foundation for Biodiversity. https://www.fondazioneslowfood.com/en/ark-of-taste-slow-food/sulmona-red-garlic/), the floral buds were removed at early stage of the emission. In late June, the whole plants were collected from crops and left to gently dry in a ventilated area, without direct sun exposure. In the following weeks, plants were carefully checked to remove unhealthy bulbs and prepared for commercialization that is in the form of whole bulbs, after removal of roots, leaves, and the outer layer of tunica, or prepared in the form of the typical garlic braids. In July 2021, the aerial bulbils (Supplementary Material) were manually isolated from the commercial batch and collected for the experiments. The bulbils belong to a representative sample of 4 Kg small size bulbils.

2.3. Extraction procedure for NMR analysis

The plant material was freeze dried in bulk for 3 days by Buchi Lyovapor 1–200 at −55 °C and 0.200 mbar until complete loss of water. Each sample was homogenized using a knife mill and was immediately subjected to Bligh-Dyer extraction protocol (Bligh and Dyer, 1959). In particular, the lyophilized sample (0.1 g) was added with 3 mL of a

Table 1
Metabolites identified in the 600.13 MHz 1H NMR spectrum of the hydroalcoholic Bligh-Dyer extract of "Sulmona Red Garlic" aerial bulbils. Asterisks indicate signals used for the integration and quantification of metabolites.

Compound	Assignment	^{1}H (ppm)	Multiplicity (J (Hz))	^{13}C (ppm)
Sugars				
α-D-Fructofuranose	CH-3	4.11		83.2
β-D-Fructofuranose	CH-4	4.12		75.6
	CH-5	3.86		81.9
α-Glucose (α-Glc)	CH-1	5.24*	d [4.0]	91.1
	CH-2	3.56		72.1
	CH-4	3.41		70.1
	CH-5	3.81		73.3
β-Glucose (β-Glc)	CH-1	4.65*	d [8.0]	96.8
	CH-2	3.28		74.9
	CH-5	3.48		76.7
	CH_2-6	3.73; 3.88		61.5
Sucrose (Suc)	CH-1 (Glc)	5.42*	d [3.8]	93.2
	CH-2	3.57		72.0
	CH–3	3.72		73.6
	CH–4	3.48		70.0
	CH–5	3.82		73.4
	CH–3′(Fru)	4.23	d [8.6]	77.8
	CH–5′	3.88		82.3
	CH–4′	3.83		61.3
	CH_2-1′	3.69		59.7
Organic Acids				
Acetic acid (AA)	α-CH_3	1.92*	s	24.6
Citric acid (CA)	α,γ-CH	2.56	d [15.1]	45.9
	α',γ'–CH	2.68*	d [15.1]	45.9
Formic acid (FA)	HCOOH	8.45*	s	
Fumaric acid (FumA)	α, β-CH = CH	6.52*	s	
Malic acid (MA)	α-CH	4.31*	dd [10.1; 3.1]	71.3
	β-CH	2.68	dd [15.5; 3.1]	43.6
	β'–CH	2.38		43.6
Pyruvic acid (PA)	CH_3	2.40*	s	30.6
Amino acids				
Alanine (Ala)	β-CH_3	1.49*	d [7.2]	17.1
	α-CH	3.80		51.3
Arginine (Arg)	α-CH	3.80		55.1
	β-CH_2	1.93	m	28.5
	γ, γ'–CH	1.73; 1.69*	m	24.9
	δ-CH_2	3.26		41.4
Asparagine (Asn)	α-CH	4.04		52.1
	β-CH	2.87*	dd [7.8; 16.9]	35.5
	β'–CH	2.98		35.5
γ-amino butyric acid (GABA)	α-CH_2	2.30*	t [7.4]	35.4
	γ-CH_2	3.03	t	40.0
Glutamate (Glu)	γ-CH_2	2.35	m	34.4
	β, β'–CH_2	2.07*, 2.13		29.9
	α-CH	3.79		55.1
Glutamine (Gln)	α-CH	3.80		55.3
	β-CH_2	2.15	m	27.0
	γ-CH_2	2.46*	m	32.6
Glycine	α-CH_2	3.57*	s	42.2
Histidine (His)	CH-5	7.17	s	117.8
	CH-2	8.07*	s	136.5
Isoleucine (Ile)	γ-CH_3	1.01*	d [7.1]	17.4
	δ-CH_3	0.89		
Leucine (Leu)	β-CH_2	1.75	m	
	δ-CH_3	0.96*	d [6.2]	21.7
	δ′–CH_3	0.97	d [6.2]	
Lysine (Lys)	α-CH	3.77		55.2
	β-CH_2	1.91	m	28.5
	ε-CH_2	3.04*	t [7.4]	40.0
Phenylalanine (Phe)	CH-2,6	7.30		130.1
	CH-4	7.37*		129.6
	CH-3,5	7.43		
Proline (Pro)	α-CH	4.15		61.7
	β, β'–CH_2	2.07, 2.37		30.0
	γ-CH_2	2.01*	m	24.7
	δ, δ′–CH_2	3.35, 3.40		47.1
Threonine (Thr)	γ-CH_3	1.33*	d [6.7]	20.2
Tryptophan (Trp)	CH-7	7.53	d [8.1]	113.2
	CH-4	7.73*	d [8.1]	119.4
Tyrosine (Tyr)	CH-2,6	7.17	d [8.6]	131.3
	CH-3,5	6.85*	d [8.6]	116.6
Valine (Val)	γ-CH_3	0.90	d [7.1]	17.6
	γ′–CH_3	1.05*	d [7.1]	18.9
Organosulphur compounds				
Alliin	CH_2-6	5.51	dq [1.2;17.0]	126.4
		5.57	*trans* dq [1.2; 10.2] *cis*	126.4
	O = S-CH_2-4	3.64; 3.87	dd	55.9
	CH_2-3	3.22; 3.44		50.9
	CH-5	5.94	m	125.5
Allicin	CH_2-6	5.51	dq [1.2;17.0]	126.4
		5.57	*trans* dq [1.2; 10.2] *cis*	126.4
	CH_2-1	5.17	dq [1.6; 10.0] *cis*	118.9
		5.21	dq [1.6; 18.6]	118.9
	O = S-CH_2-4	3.64; 3.87	*trans* dd	55.9
	CH-2	5.84*	m	134.7
	CH-5	5.94	m	125.5
	S-CH_2-3	3.24	dd	41.3
Cycloalliin	CH_3	1.44*	d [6.5]	19.5
	O = S-CH_2-6	2.81; 3.23		47.7
	N-CH-5	3.93		43.7
S-Methyl-L-cysteine-S-oxide (Methiin, MCSO)	γ-CH_3	2.83*	s	39.1
	β-CH_2	3.27, 3.47		54.0
	α-CH	4.18		59.3
Sulphur compounds (OSCs)	CH_2 = CH–	5.99	dq	122.3
Miscellaneous				
Choline	$N(CH_3)_3$	3.20*	s	54.9
Glycine betaine	$N(CH_3)_3$	3.27*	s	54.4
	α-CH_2	3.81		67.3
Pyroglutamic acid	β, β'–CH_2	2.04, 2.51*	m	26.5
	γ-CH_2	2.40		32.5
Trigonelline	CH-6	9.13*	s	
	CH-4,2	8.84		
Tyramine	CH-3,5	7.21		131.6
	CH-2,6	6.90*	d	116.6
Uridine	CH-1′ (rib)	5.90		
	CH-6	7.88*	d [7.9]	

d = doublet; dd = doublet of doublets; dq = doublet of quartet; m = multiplet; s = singlet; t = triplet.

$CH_3OH/CHCl_3$ mixture (2:1 v/v) and 0.8 mL of double-distilled water. The resulting system was sonicated at room temperature for 10 min, followed by the addition of 1 mL of chloroform and 1 mL of double-distilled water. The hydroalcoholic and organic phases were finally separated after centrifugation (Eppendorf Centrifuge 5430 R (Milan, Italy)) for 15 min (25 °C, 7540 g). The residual pellets were extracted two more times under the same conditions as described. The three extractions obtained from each step were combined. The hydroalcoholic fraction were dried using nitrogen flow. The dried extracts were stored at − 20 °C until further analysis.

2.4. NMR analysis

NMR analyses were carried out on a Jeol JNM-ECZ 600R operating at the proton frequency of 600.17 MHz and equipped with a Jeol 5 mm FG/RO DIGITAL AUTOTUNE probe. ^{1}H NMR experiments were carried out

Table 2
Gradient elution condition of HPLC-DAD analyses of the hydroalcoholic extract of "Sulmona Red Garlic" bulbils.

TIME (min)	COMPOSITION A% (Water + Formic acid 0.1 %)	COMPOSITION B% (Methanol + Formic acid 0.1 %)	FLOW (mL/min)
1	97	3	0.6
5	77	23	0.6
12	73	27	0.6
18	57	43	0.6
25	52	48	0.6
32	50	50	0.6
34	50	50	0.6
37	35	65	0.6
40	5	95	0.6
47	10	90	0.6
48	10	90	0.6

by using the following parameters: 298 K, 128 scans, residual water signal suppression with a presaturation pulse, 7.73 s relaxation delay, 90° pulse of 8.3 μs, 64 k data points, and 9000 Hz spectral width. Homonuclear ^{1}H–^{1}H TOCSY experiment was acquired with 64 scans, 8 k data points in f_2 and 128 in f_1, 50 ms mixing time, 2 s relaxation delay, and 9000 Hz spectral width in both dimensions. Heteronuclear ^{1}H–^{13}C HSQC experiment was acquired with 64 scans, 8 k data points in f_2 and 256 in f_1, 2 s relaxation delay, and a spectral width of 9000 Hz and 33000 Hz for f_2 and f_1, respectively (Spano et al., 2023) (Spano, M.; Di Matteo, G.; Fernandez Retamozo, C.A.; Lasalvia, A.; Ruggeri, M.; Sandri, G.; Cordeiro, C.; Sousa Silva, M.; Totaro Fila, C.; Garzoli, S.; et al. A Multimethodological Approach for the Chemical Characterization of Edible Insects: The Case Study of *Acheta domesticus*. *Foods* **2023**, *12*, 2331. https://doi.org/10.3390/foods12122331).

The dried hydroalcoholic phase was dissolved in 700 μL of 100 mM phosphate buffer/D_2O, containing 0.4 mM TSP as internal standard. ^{1}H spectra were referenced to methyl group signals of TSP ($\delta_H = 0.00$ ppm) in D_2O. Spectra processing, and signals integration were carried out with JEOL Delta software (v5.3.1).

Metabolite quantification was carried out by integration of selected signals (marked with asterisk) listed in Table 1 using JEOL Delta software (v5.3.1) and normalized with respect to the methyl group signal of TSP (0.00 ppm), set to 100. The quantified metabolites were expressed as mg/100 g of dried sample. NMR chemical shift used for signal integration are reported with an asterisk in Table 1.

2.5. Extraction procedure for phenolic HPLC analysis and biological studies

Extracts for phenolic analysis and biological studies were prepared according to a protocol already described (Lasalvia et al., 2022; Recinella et al., 2022). In particular, the extraction was performed by maceration in a sonicator bath at a frequency of 30 kHz [2 consecutive extractions of 30 min each at room temperature (20 °C)] with water–ethanol (50:50, v/v). The plant material/solvent ratio was 1/20 (w/w). The extract was freshly prepared and centrifuged at 5000g (Menghini et al., 2018).

2.6. HPLC determination of phenolic compounds

The quantitative determination of phenols present in the water–ethanol (50:50, v/v) extract was carried out using a reversed-phase HPLC-DAD in gradient elution mode as previously described (Acquaviva et al., 2022). Phenols separation was conducted within 60 min of the chromatographic run, starting from the following separation conditions: 97 % water with 0.1 % formic acid, 3 % methanol with 0.1 % formic acid (Table 2). The separation was performed on an Infinity lab Poroshell 120-SB reverse phase column (C18, 150 × 4.6 mm i.d., 2.7 μm; Agilent, Santa Clara, CA, USA). Column temperature was set at 30 °C. Quantitative determination of phenolic compounds was performed via a DAD detector. Quantification was done through 7-point calibration curves, with linearity coefficients (R^2) > 0.999, in the concentration range 2–140 μg/mL. All standards were purchased from Sigma Aldrich (Milan, Italy), and have a purity ≥ 95 %. The limits of detection were lower than 1 μg/mL for all assayed analytes. The area under the curve from HPLC chromatograms was used to quantify the analyte concentrations in the extract.

2.7. Eco-toxicological studies

Allelopathy bioassay was carried on the seeds of the herbaceous dicotyledon species *Cichorium intybus* and *C. endivia* because of their fast germination rate and high sensitivity. The detailed procedure was conducted as previously reported (Ferrante et al., 2019). Seeds were treated with scalar *A. sativum* extract concentrations (0.625–40 mg/mL) and considered germinated for observed root length ≥ 1 mm, after the third day of treatment. *Artemia salina* (brine shrimp) was cultured as previously described (Orlando et al., 2021), and toxicity induced by the extract (0.1–20 mg/mL) was expressed in terms of LC_{50} values. *Daphnia magna* were cultured as previously described (Villegas-Navarro, Rosas-L, & Reyes, 2003). Briefly, non-pregnant *Daphnia magna* were maintained separately in 50 mL of extract solution (10 mg/mL) at room temperature throughout the experiment. The hearth rate was recorded through microscopy. *Daphnia magna* were placed individually onto a single cavity microscope slide in a 50 μL droplet of the tested extract, where the heartbeat rate was measured three times for 10 s. Each measurement was conducted in triplicate. The decrease in hearth rate was compared to both untreated and 30 % ethanol-treated groups, working as negative and positive controls, respectively.

2.8. In vitro study

2.8.1. Human cardiomyocyte C2C12 cell line

Human cardiomyocyte C2C12 cell line was cultured in DMEM (Euroclone) supplemented with 10 % (v/v) heat-inactivated fetal bovine serum and 1.2 % (v/v) penicillin G/streptomycin in 75 cm^2 tissue culture flask (n = 5 individual culture flasks for each condition). The cultured cells were maintained in humidified incubator with 5 % CO_2 at 37 °C. For cell differentiation, C2C12 cell suspension at a density of 1 × 10^6 cells/mL was treated with various concentrations (10, 50, and 100 ng/mL) of phorbol myristate acetate (PMA, Fluka) for 24 h or 48 h (induction phase). Thereafter, the PMA-treated cells were washed twice with ice-cold pH 7.4 phosphate buffer solution (PBS) to remove PMA and non-adherent cells, whereas the adherent cells were further maintained for 48 h (recovery phase). Morphology of cells was examined under an inverted phase-contrast microscope. To assess the basal cytotoxicity of the extract, a viability test was performed on 96 microwell plates, using 3-(4,5-dimethylthiazol-2-yl)-2,5-diphenyltetrazolium bromide (MTT) test. Cells were incubated with the extract (ranging in the concentration 10–1000 μg/mL) for 24 h. 10 μL of MTT (5 mg/mL) was added to each well and incubated for 3 h. The formazan dye formed was extracted with dimethyl sulfoxide and absorbance was recorded as previously described (Menghini et al., 2018). Effects on cell viability was evaluated in comparison to untreated control group (Ctrl).

2.8.2. Human colon cancer-derived HCT116 cell

Human colon cancer-derived HCT116 cell were cultured in DMEM (Euroclone) supplemented with 10 % (v/v) heat-inactivated fetal bovine serum and 1 % (v/v) penicillin G/streptomycin in a 75 cm^2 cell culture flasks. The cultured cells were maintained in a humidified incubator with 5 % CO_2 at 37 °C. When the confluency reached 80 %, a viability test was performed using 3-(4,5-dimethylthiazol-2-yl)-2,5-diphenyltetrazolium bromide (MTT) test to assess the basal cytotoxicity of the extract under investigation. For this assay cells were seeded (5x10^3 cells/well) onto flat-bottomed 96-well culture plates and incubated

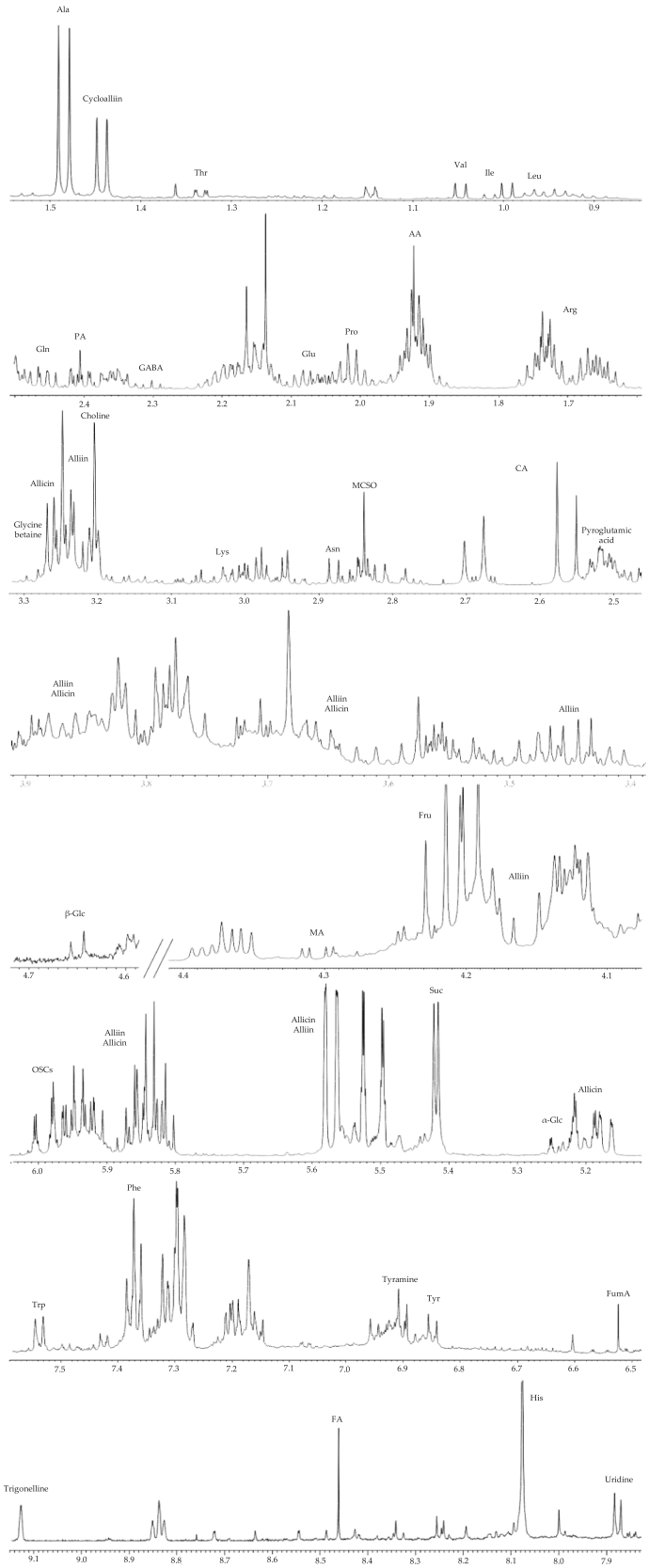

Fig. 1. ^{1}H NMR spectrum of the hydroalcoholic Bligh-Dyer extract, in 100 mM PBS/D_2O, 0.4 mM TSP.

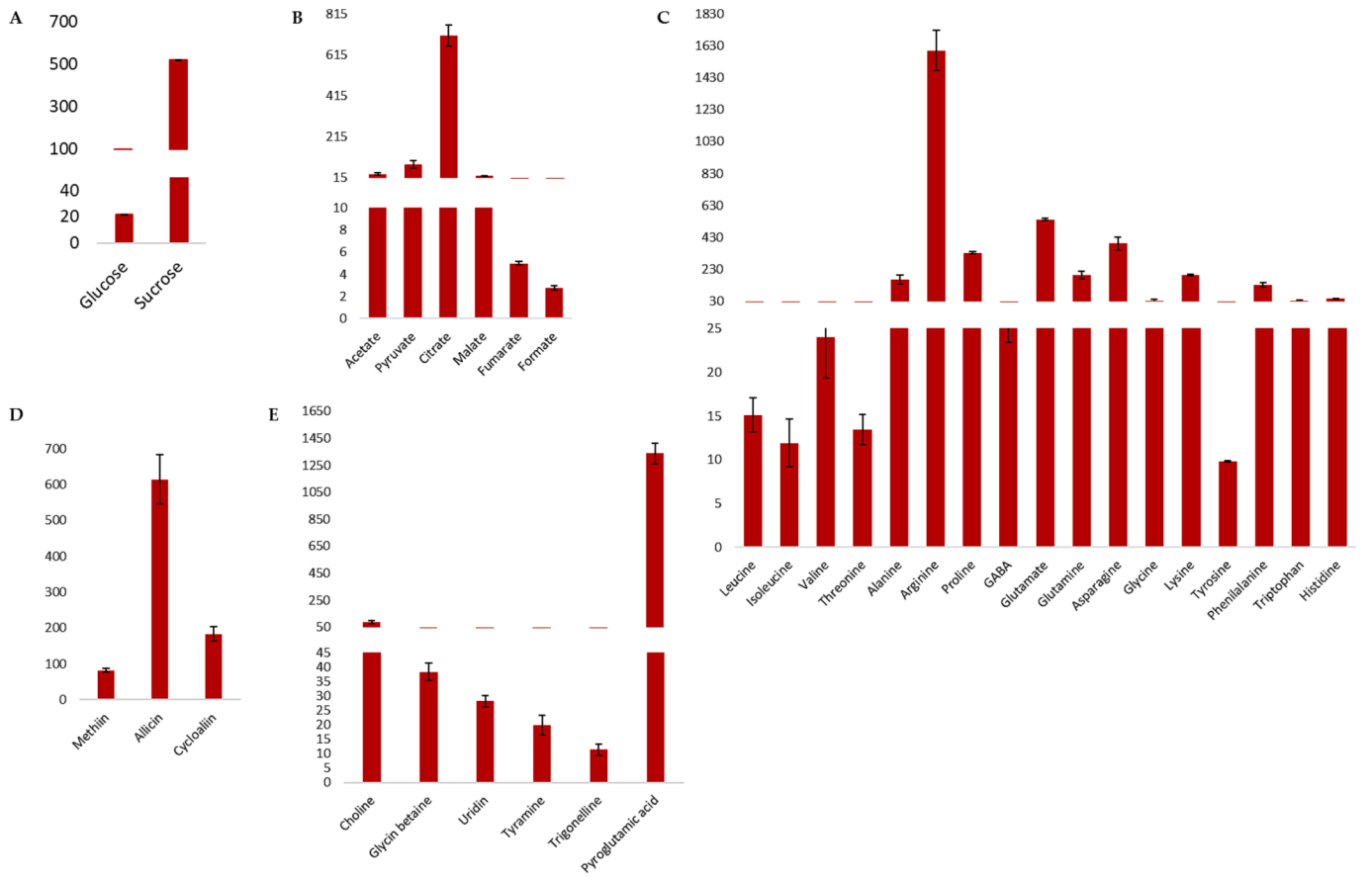

Fig. 2. Histograms resulting from the quantitative NMR analysis of quantified compounds (mg/100 mg dry weight) present in the Bligh-Dyer hydroalcoholic extracts of red garlic aerial bulbils. (A) Sugars, (B) Organic acids, (C) Amino acids, (D) Organosulphur compounds, and (E) Miscellaneous. (For interpretation of the references to colour in this figure legend, the reader is referred to the web version of this article.)

overnight. After 24 h, the extract at different concentrations (200–1000 μg/mL) was added and the plates were incubated for 24 h. After this time, a total of 10 μL of MTT (5 mg/mL in PBS) was added to each well and incubated for 3 h. The formazan dye formed was solubilized with dimethyl sulfoxide and absorbance was recorded at 540 nm. Effects on cell viability were evaluated in comparison to the control (Ctrl: untreated cells) and expressed as a percentage of the control culture value. In a second set of experiments cells were treated with either vehicle or extract for 24 h and subsequently post-treated with hydrogen peroxide (H.P.) 300 μM for 3 h. After this time, cell survival was determined by MTT assay as described above. Each condition was run in triplicate, including untreated control and blank cell-free control.

Total RNA was extracted from HCT116 cells using TRI reagent (Sigma-Aldrich, St. Louis, MO, USA), according to the manufacturer's protocol, and reverse transcribed using High-Capacity cDNA Reverse Transcription Kit (Thermo Fischer Scientific, Waltman, Massachusetts, USA). Gene expression of TNFα, TRPM8, HIF1α, and VEGFA were determined by quantitative real-time PCR using TaqMan probe-based chemistry, as previously described (Menghini et al., 2018). PCR primers and TaqMan probes were purchased from Thermo Fisher Scientific Inc. β-actin was used as the house-keeping gene. The elaboration of data was conducted with the Sequence Detection System (SDS) software version 2.3 (Thermo Fischer Scientific). Relative quantification of gene ex-pression was performed by the comparative $2^{-\Delta\Delta Ct}$ method (Livak & Schmittgen, 2001).

2.9. In silico predictions and molecular modelling

The putative targets and pathways underlying the mechanism of action of the extract were predicted through the bioinformatics platform STITCH (accessed on 11th April 2023), as previously described (Ferrante et al., 2020; Gu et al., 2020).

The cryo-EM structure of the TRPM8 ion channel complexed with icilin was retrieved from the protein data bank (PDB ID: 6NR3) (https://www.rcsb.org/) (accessed on 18th February 2023). The protein was prepared using Playmolecule web server (https://playmolecule.com/proteinPrepare/) (accessed on 18th February 2023) (Martínez-Rosell, Giorgino, & De Fabritiis, 2017). The 3D structure of alliin was retrieved from the PubChem database (https://pubchem.ncbi.nlm.nih.gov/) (accessed on 18th February 2022) and its geometry was optimized using Biovia Discovery Studio Visualizer v4.5 (Dassault Systèmes Biovia Software Inc, San Diego, CA, USA, 2012). The binding coordinates of the cocrystal ligand icilin were used to define the docking grid box x, y, z dimension (50, 50, 50 Å) and x, y, z center coordinates (171.7, 137.5, 174.9 Å) with 0.375 Å using AutoDockTools 1.5.6. Docking was carried out using AutoDock 4.2.6 (https://autodock.scripts.edu) (Morris et al., 2009). The docking protocol, including the algorithm and the number of energy evaluations, have been previously described (Albayati, Uba, & Yelekçi, 2022; Llorent-Martínez et al., 2022). The docking score of each ligand pose was calculated, and protein–ligand interaction was analyzed using Biovia Discovery Studio Visualizer v4.5 (Dassault Systèmes Biovia Software Inc, San Diego, CA, USA, 2012).

2.10. Statistical analysis

The software GraphPad Prism version 5.01 (Graphpad Software Inc., San Diego, CA, USA) was used to perform data analysis. Means ± SD

were determined for each experimental group and analyzed by ANOVA, followed by Newman-Keuls multiple comparison post hoc test. The limit of statistically significant differences between mean values was set at p-value < 0.05.

3. Results and discussion

3.1. 3.1 Metabolomic profile of bulbils aqueous extract by NMR analysis

The ^{1}H spectrum of Bligh-Dyer hydroalcoholic extracts from "Sulmona Red Garlic" bulbils, see Fig. 1, was assigned using 2D NMR experiments (^{1}H–^{1}H TOCSY, ^{1}H–^{13}C HSQC) and literature data on other vegetable food matrices (Ingallina et al., 2023; Liang et al., 2015; Ritota et al., 2012; Saviano et al., 2019; Spano et al., 2021). In some specific cases, the comparison with the NMR spectra of pure reference standard were also carried out to confirm the compound assignment.

In the high-field 0.8–3.6 ppm spectral region, signals of methyl and methylene groups belonging to aliphatic amino acids and organic acids are observed. The spectral region between 3.0 ppm 5.5 ppm is dominated by very intense signals of principal monosaccharides and disaccharides, and organosulphur compounds.

In the low frequency spectral region (6.0–9.0 ppm), ^{1}H signals of amino acid aromatic groups (phenylalanine, tryptophan, and tyrosine), formic and fumaric acids and trigonelline, uridine and tyramine were detected.

Hereunder, each class of compounds is discussed separately.

3.1.1. Sugars

The ^{1}H NMR spectrum revealed the presence of mono- and disaccharides characterized by distinct ^{1}H resonances due to anomeric CH-1 group: β-D-glucose and α-D-glucose signals at 5.24 ppm and 4.65 ppm, sucrose and fructose signal at 5.42 ppm and 4.11 ppm, respectively. Sucrose and glucose were quantified showing a content of 518.98 ± 0.89 and 21.50 ± 0.29 mg, respectively (Fig. 2**A**).

This class of metabolites play a key role in the physiological activities of bulbils over to ensure the basal metabolism of autotrophic cells. In garlic, and generally in plants, sugars act as a carbohydrate reserve and soluble molecules able to modulate osmoregulation and prevent cell damage. They are usually mobilized and used from plant during growth phases and sprout development.

3.1.2. Organic acids

^{1}H NMR spectrum showed the presence of acetic, pyruvic, citric, malic, fumaric and formic acids. The presence of acetic acid was confirmed by the methyl group singlet at 1.92 ppm and the relative correlation with carbon atom at 24.6 ppm in the ^{1}H–^{13}C HSQC spectrum.

The singlet at 2.40 ppm which correlate with carbon at 30.6 ppm referred to methyl group of pyruvic acid. Citric acid was identified by the typical doublets ($J_{H\text{-}H}$ = 15.1 Hz) at 2.56 and 2.68 ppm of the symmetric diastereotopic CH_2 groups that correlated with carbon at 45.9 ppm in ^{1}H–^{13}C HSQC spectrum. Citrate is a clavation products of amino acids and, with sulfur compounds, allows to define the sensory profile of bulbs and bulbils (Jones et al., 2004).

According with literature (Liang et al., 2015; Ritota et al., 2012) also malic acid was found due to the presence of double doublets ($J_{H\text{-}H}$ = 10.1 and 3.1 Hz) at 4.31 ppm corresponding to the α-CH proton. The cross-peaks in ^{1}H–^{1}H TOCSY experiment showed the mutual correlation with β-CH (2.68 ppm) and β'–CH (2.38 ppm) protons. Moreover, the ^{1}H–^{13}C HSQC spectrum confirmed the short-range correlation between each proton with corresponding carbons at 71.3 and 43.6 ppm, respectively. Malate could not be quantified by the integration of β-CH_2 doublets due to their poor resolution being overlapped with one doublet (2.68 ppm) of citrate, thus the signal at 4.31 ppm had been chosen for integration. Both fumaric and formic acids were identified by the presence of the typical singlets at 6.52 ppm and 8.45 ppm, respectively. The most abundant organic acid turned out to be citrate (over 700 mg/100 g DW), followed by pyruvate, acetate, and malate, above 100 mg/100 g DW (Fig. 2**B**). Fumaric and formic acids were found in very low concentrations, below 5 mg/100 g dry weight matrix.

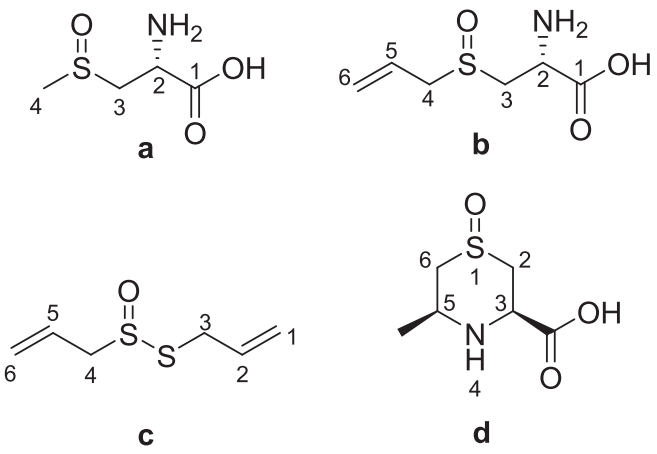

Fig. 3. Structures of organosulphur compounds: (a) methiin; (b) alliin; (c) allicin; (d) cycloalliin.

3.1.2.1. Amino acids. Seventeen amino acids, namely alanine, arginine, asparagine, GABA, glutamic acid, glutamine, glycine, histidine, isoleucine, leucine, lysine, phenylalanine, proline, threonine, tyrosine, tryptophan, and valine were identified in the ^{1}H spectrum. In addition to GABA, two other non-protein amino acids, namely methiin and alliin, typically found in vegetables of Brassicaceae and Liliaceae (Amaryllidaceae) family, were also identified. Their assignment will be discussed in (3.1.4) section together with the other organosulfur compounds.

Signals in the range from 0.90 to 1.10 ppm arise from methyl or methylene groups of valine, leucine, and isoleucine, ^{1}H–^{1}H and TOCSY correlations allowed the correct assignment. The multiplet at 1.69 ppm and its correlation with the carbon at 24.9 ppm in the ^{1}H–^{13}C HSQC represented the typical spin pattern of γ'–CH of arginine. α-CH (^{1}H 3.80 and ^{13}C 55.1 ppm), β-CH_2 (^{1}H 1.93 and ^{13}C 28.5 ppm), γ-CH (^{1}H 1.73 ppm and ^{13}C 24.9), and δ-CH_2 (^{1}H 3.26 and ^{13}C 41.4 ppm) signals were assigned by means of ^{1}H–^{1}H TOCSY and ^{1}H–^{13}C HSQC experiments.

Arginine turned out to be the most abundant amino acid, as nitrogen reserve stored in the roots to ensure plant growth during germination and budbreak (Gomez, Vercambre, & Jordan, 2020; Keller & Senula, 2013; Yang et al., 2017).

3.1.2.2. Organosulphur compounds. As reported in literature (Putnik et al., 2019, Block, 1992) garlic bulbs, contain major organosulphur compounds (OSCs), namely γ-glutamylcysteines, non-protein amino acids, and their corresponding sulfoxide derivatives, being (+)-S-(2-propenyl)-L-cysteine sulfoxide (alliin), (+)-S-(*trans*-1-propenyl)-L-cysteine sulfoxide (isoalliin), and (+)-S-methyl-L-cysteine sulfoxide (methiin), (1S,3R,5S)-5-methyl-1,4-thiazane-3-carboxylic acid 1-oxide (cycloalliin), and S-(Prop-2-en-1-yl) prop-2-ene-1-sulfinothioate (allicin) the principal ones (Borlinghaus et al., 2014).

The ^{1}H NMR spectrum of bulbils extracts show the presence of four organosulphur compounds namely allicin, methiin, and alliin and cycloalliin, see Fig. 3. In order to simplify the discussion about the assignment, the numbering of allicin will not adhere to the IUPAC standard. This is to ensure that the identical part of the molecule between allicin and alliin has the same numbering. According to the IUPAC numbering rules, the allyl-sulfoxide group should have priority. However, as shown in Fig. 3, the C atoms in allicin have been numbered starting from the allyl-sulfino group. Here for the first time, it is reported the assignment of methiin, and alliin in the ^{1}H spectrum of aerial bulbil garlic extracts. Methiin naturally occurring in the genus *Allium*, with

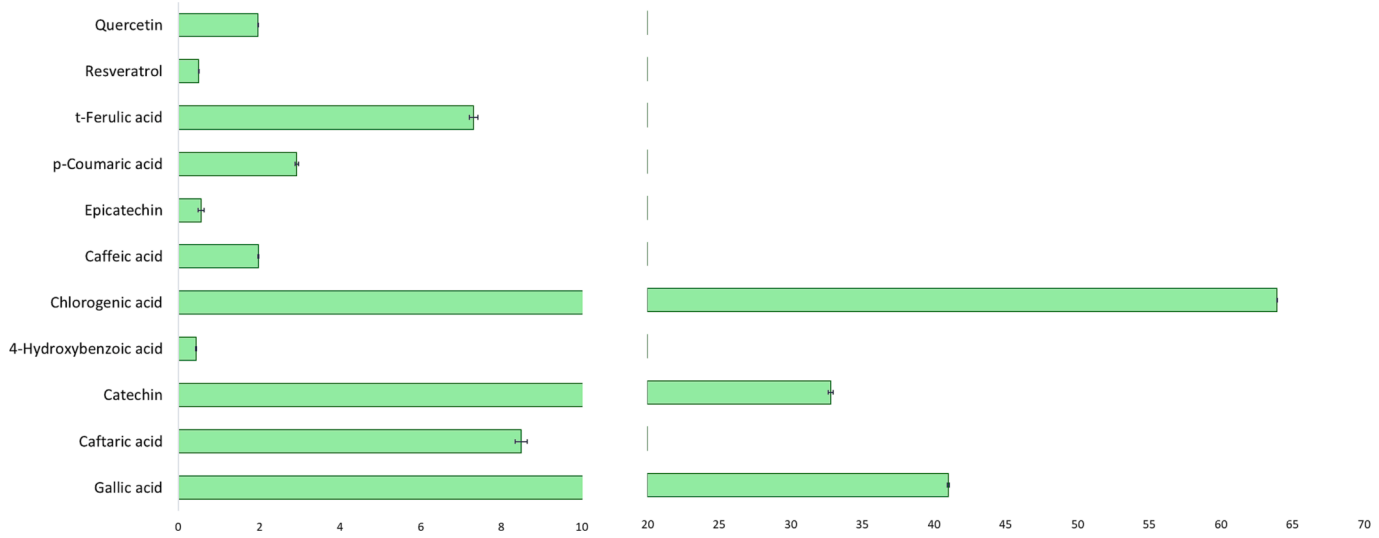

Fig. 4A. Histograms relative to concentration (mg/100 g) of phenolic compounds in the red garlic aerial bulbil hydroalcoholic extract. (For interpretation of the references to colour in this figure legend, the reader is referred to the web version of this article.)

regards to *sativum* species (Rose et al., 2005), and some members of Brassicaceae, like *Brassica oleracea* L. (Ingallina et al., 2023) was identified by means of the spin correction observed in the ^{1}H–^{1}H TOCSY map between the α-CH (^{1}H 4.18 ppm, ^{13}C 59.3) and diastereotopic protons of β-CH_2 (^{1}H 3.27, 3.47 ppm, ^{13}C 54.0 ppm). The assignment of γ-CH_3 group linked to the -S = O group 2.83 ppm (^{13}C 39.1 ppm) was confirmed by literature data regarding other vegetable matrices (Saviano et al., 2019).

With regards to alliin and allicin, the two major allyl-sulphur metabolites, signals arising from allyl-organosulphur compounds were observed in spectral region between 5.00 and 6.00 ppm of the ^{1}H NMR spectrum. In particular, the multiplet at 5.94 ppm (^{13}C 125.5 ppm) assigned to the proton of CH-5 showed in the ^{1}H–^{1}H TOCSY map a spin correlation with: the protons of methylene CH_2-6 at 5.57 ppm (dq $J_{H\text{-}H}$ = 1.2 Hz and $J_{H\text{-}Hcis}$ = 10.2 Hz) and 5.51 ppm (dq $J_{H\text{-}H}$ = 1.2 Hz and $J_{H\text{-}Htrans}$ = 17.0 Hz), and the diastereotopic methylene protons next to -S = O group at 3.64 and 3.87 ppm (^{13}C 55.9 ppm) accounted for the CH_2-4. The second spin system of alliin is analogue to the methiin. However, the ^{1}H–^{13}C HSQC spectrum showed a short-range correlation between the signals of diastereotopic methylene protons at 3.22 and 3.44 ppm and the corresponding carbon at 50.9 ppm, which accounted for the CH_2-3. These signals belong, most likely, to alliin, as confirmed by comparison with the ^{1}H, ^{13}C and ^{1}H–^{13}C HSQC spectra of the reference standard and literature data (Hakamata et al., 2015). The presence of allicin was assessed by the evidence of a further spin system consisting of the double bond methines at 5.17 (dq $J_{H\text{-}H}$ = 1.6 Hz and $J_{H\text{-}Hcis}$ = 10.0 Hz), 5.21 (dq $J_{H\text{-}H}$ = 1.6 Hz and $J_{H\text{-}Htrans}$ = 18.6 Hz) and a multiplet at 5.84 ppm, corresponding to CH_2-1 and CH-2, respectively. These signals showed a ^{1}H–^{13}C HSQC short-range correlation with the carbon at 118.9 and 134.7 ppm, respectively, and a ^{1}H–^{1}H TOCSY spin-correlation with methylene protons S-CH_2-3 (^{1}H 3.24 and ^{13}C 41.3 ppm). Signals belonging to the second part of the molecule overlapped in the ^{1}H spectrum with the signals from alliin, and their assignment was based on 2D experiment and the literature data (Ritota et al., 2012; Liang et al., 2015).

Cycloalliin assignment was based on the presence of the characteristic doublet signal at 1.44 ppm ($J_{H\text{-}H}$ = 6.5 Hz) from the protons of the -methyl substituent in C-5, which showed a short-range correlation in the ^{1}H–^{13}C HSQC spectrum with the carbon at 19.5 ppm. Moreover, in the ^{1}H–^{1}H TOCSY spectrum, cross-peak correlations between the methyl substituent in C-5 and the proton at 3.93 ppm (^{13}C 43.7 ppm), which accounted for the α proton CH-5, and protons at 2.81 and 3.23 ppm, assigned to the methylene CH_2-6 (^{13}C 47.7 ppm) next to sulfoxide group were observed. These findings agreed with the literature data (Liang et al., 2015). The absence of isoalliin in the ^{1}H NMR spectrum could be due to its exclusive biosynthesis in species of *Allium cepa*. (Borlinghaus et al., 2014). All the organosulphur compounds were identified and quantified (Fig. 2**D**), with the exception of alliin. This is due to the significant overlap of its characteristic signals with those of allicin and methiin.

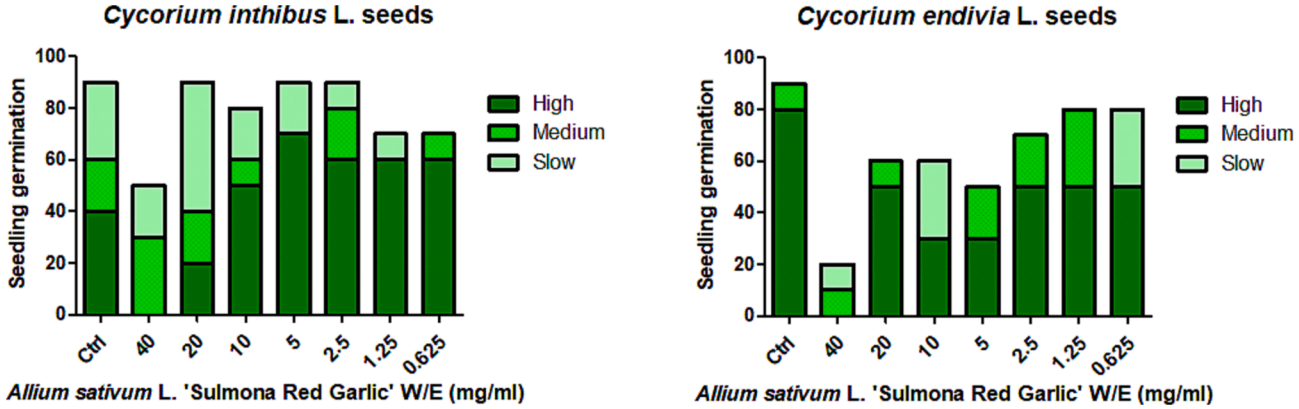

Fig. 5. Effects of the hydroalcoholic extract of aerial bulbils from "Sulmona Red Garlic" on the seedling germination of *Cycorium inthibus* and *Cycorium endivia*.

Table 3
Content in metabolites (μg/mL) of the red garlic aerial bulbil hydroalcoholic extract. All identified phytochemicals have been identified through comparison with pure standards. Quantitative determination of the compounds was performed via DAD detector at 232–372 nm wavelength; nq: not quantified; nd: not detected.

	Phytochemical	Rt	Wavelength	Concentration
1	Gallic acid	8.80	271	16.400 ± 0.059
2	3-Hydroxytyrosol	11.71	275	nq
3	Caftaric acid	12.93	310	3.397 ± 0.147
4	Catechin	14.80	278	13.118 ± 0.163
5	4-Hydroxybenzoic acid	16.20	256	0.176 ± 0.012
6	Chlorogenic acid	16.81	325	25.573 ± 0.010
7	Vanillic acid	18.60	257	nq
8	Caffeic acid	19.00	325	0.790 ± 0.011
9	Epicatechin	19.41	278	0.226 ± 0.078
10	Syringic acid	20.05	274	nd
11	Syringaldehyde	21.80	310	nq
12	p-Coumaric acid	23.06	310	1.170 ± 0.045
13	t-Ferulic acid	24.00	315	2.925 ± 0.105
14	Hyperoside	26.92	254	nq
15	Rutin	27.16	254	nq
16	Resveratrol	27.70	310	0.202 ± 0.002
17	t-Cinnamic acid	34.39	279	nq
18	Quercetin	35.89	372	0.785 ± 0.006
19	Kaempferol	41.74	330	nq
20	Carvacrol	44.69	275	nd
21	Flavone	45.60	340	nq
22	3-Hydroxyflavone	46.05	340	nq
23	Emodin	47.70	289	nq

3.1.3. Miscellaneous

^{1}H NMR spectrum revealed the presence of other metabolites reported in Table 1. According to Liang et al (Liang et al., 2015), pyroglutamic acid was identified due to the resonance of the diastereotopic protons β, β'–CH_2 at 2.04 and 2.51 ppm, respectively (^{13}C 26.5 ppm). This signal showed in the ^{1}H–^{1}H TOCSY map a spin correlation with γ-CH_2 protons at 2.40 ppm (^{13}C 32.5 ppm). Resonance at 9.13 ppm showed a ^{1}H–^{1}H TOCSY cross-peak with proton at 8.84 ppm and was assigned to trigonelline, in accordance with data reported in literature (Ritota et al., 2012). Singlet at 3.27 ppm showing a correlation in ^{1}H–^{1}H TOCSY with proton at 3.81 ppm (α-CH_2) was attributed to the $+N(CH_3)_3$ methyl groups of glycine betaine. Its presence was also confirmed by the ^{1}H–^{13}C HSQC spectrum, which yield correlations between each proton with their carbons at 54.4 and 67.3 ppm, respectively. Also, tyramine was identified based on the presence of the characteristic doublet at 6.90 ppm assigned to CH-2,6. This signal showed in the ^{1}H–^{1}H TOCSY experiment a correlation with protons CH-3,5 at 7.21 ppm. The ^{1}H–^{13}C HSQC allowed the short-range correlation between these protons with corresponding carbons at 116.6 and 131.6 ppm, respectively. Finally, according to literature, choline and uridine were identified in the hydroalcoholic extract of Sulmona Red Garlic aerial bulbils. In detail, singlet at 3.20 ppm was attributed to choline, whereas the presence of uridine was assessed by the presence of the doublet at 7.88 ($J_{H\text{-}H}$ = 7.9 Hz), assigned to CH-6, which correlated in the ^{1}H–^{1}H TOCSY spectrum with the CH-1′ proton at 5.90 ppm (Fig. 2**E**).

3.2. Phenolic compounds by HPLC-DAD analysis

The hydroalcoholic extract of garlic aerial bulbils was also assayed through HPLC-DAD to obtain the phenolic quantification. The experimental data are reported in Figs. 4A and Fig. 4B and Table 3 that showed gallic acid, catechin, and chlorogenic acid as the prominent phytochemicals. These compounds were present at concentrations ranging from 13.118 to 25.573 μg/mL, and this is consistent, albeit partially, with literature (Recinella et al., 2022). On the other hand, *t*-ferulic and caftaric acid ranged from 2.925 and 3.397 (μg/mL), respectively. Collectively, the extract's concentration of the present phytochemicals is consistent with potential antioxidant and anti-inflammatory effects (Chiavaroli et al., 2021; Recinella et al., 2022); thus, further supporting the pharmacological evaluation described below.

3.3. Eco-toxicological studies

In order to validate the bio-pharmacological use of the hydroalcoholic extract from the aerial bulbils of the "Sulmona Red Garlic" ecotype, a multidirectional ecotoxicological approach was conducted in

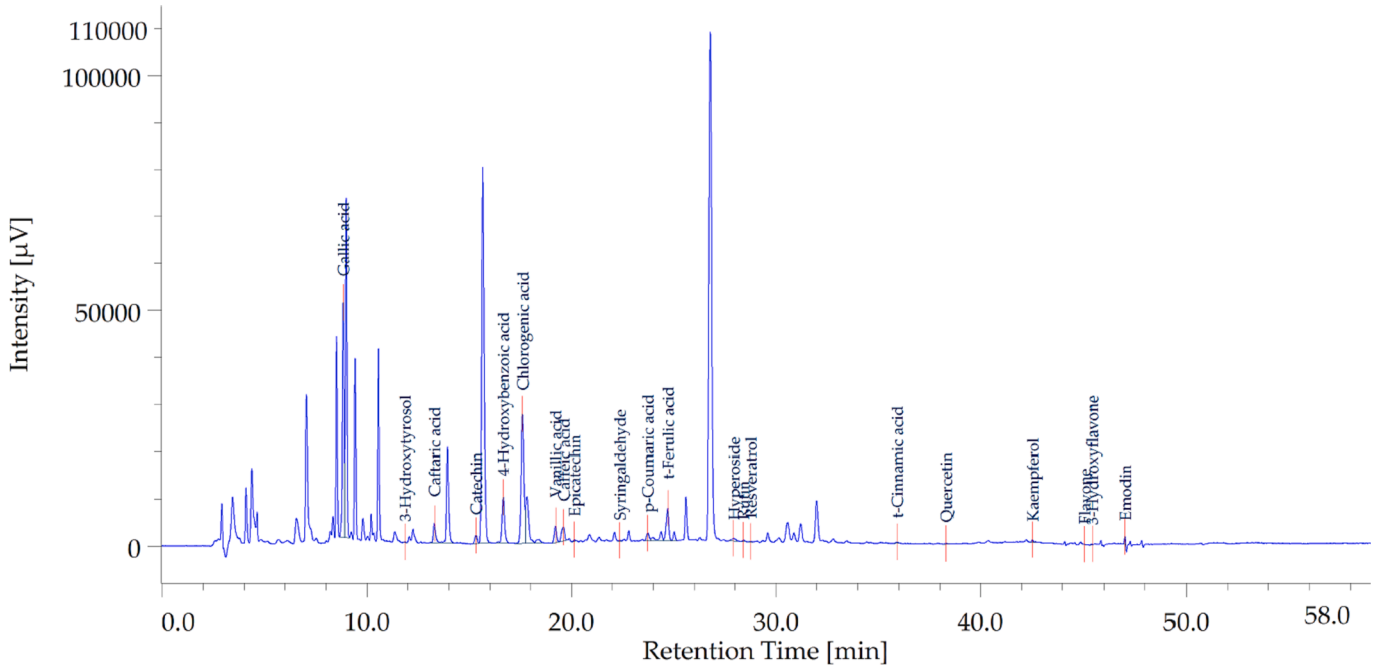

Fig. 4B. Chromatographic analysis of the phenolic compounds present in the hydroalcoholic extract from the aerial bulbils of "Sulmona Red Garlic". Among the identified phytochemicals, the prominent were: gallic acid, caftaric acid, catechin, chlorogenic acid, and t-ferulic acid. (For interpretation of the references to colour in this figure legend, the reader is referred to the web version of this article.)

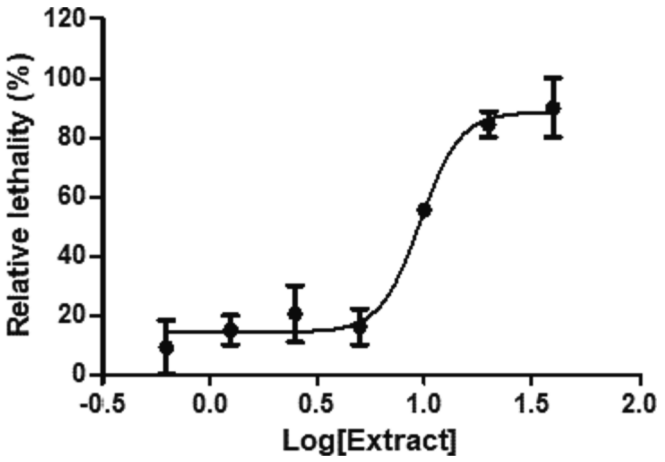

Fig. 6. Effect of the hydroalcoholic extract of aerial bulbils from "Sulmona Red Garlic" on the viability of the *Artemia salina* (Brine shrimp lethality assay). LC_{50}: 9.581 mg/mL.

order to discriminate the limits of biocompatibility in eukaryotic organisms. In this regard, a former investigation was carried out to study the phytotoxicity of the extract against two edible and herbaceous dicotyledon species, namely *Cichorium intybus* and *C. endivia.* The seedling germination was evaluated for both of them, after exposing the seeds to the extract (0.625–40 mg/mL). The extract caused a significant reduction (over 50 %) of the seedling germination at the highest tested concentration that was considered phytotoxic (Fig. 5). This is consistent, albeit partially, with the extract content in phenolic compounds that are well-known to work as allelochemicals (Dehghanian et al., 2022). In parallel, the effects of the extract on the survival of the *Artemia salina* (brine shrimp) was evaluated, as well. In this context, the extract was tested in the same concentration range (0.625–40 mg/mL). As already observed for polar extracts prepared with ultrasound-assisted maceration from other edible plants (Chiavaroli et al., 2021; Orlando et al., 2021) a LC_{50} value ≈ 10 mg/mL was provided by the brine shrimp lethality test (Fig. 6). This LC_{50} value was therefore chosen as concentration limit for the *Daphnia magna* toxicity assay. In this in vitro model, the extract did not influence the heart rate of the *D. magna* in both basal and ethanol-induced toxicity conditions (Fig. 7); thus, suggesting a different sensitivity of the *D. magna* to the extract, compared with *A. salina.* In agreement with previous studies (Chiavaroli et al., 2021; Orlando et al., 2021), a concentration at least ten-fold lower than the LC_{50} calculated with brine shrimp lethality assay was chosen as putative biocompatibility limit for the in vitro assays described below.

3.4. In vitro studies

The garlic extract (200–1000 μg/mL) was also tested on colon cancer HCT116 cell line, for studying cytotoxicity properties. In parallel, the extract was assayed on the myocyte C2C12 cell line, chosen as non-tumoral comparison cell line. Intriguingly, the two cell lines showed a different sensitivity to the extract; indeed, C2C12 cells tolerated the extract up to the concentration of 1000 μg/mL (Fig. 8**A**); thus, demonstrating a good biocompatibility as expected from the abovementioned eco-toxicological models. By contrast, the extract determined a significant and concentration-dependent reduction of HCT116 cell viability (Fig. 8B-C), starting from the concentration of 200 μg/mL, that adds, albeit partially, to recent in vitro and in vivo findings (Ansary et al., 2020; Recinella et al., 2022; Tanrıkulu et al., 2020).

In HCT116 cells, the gene expression of different factors involved in angiogenesis, cell migration, and inflammation-to-cancer transition, namely TNFα, HIF1α, and VEGFA (Chen et al., 2019; Panyathep, Punturee, & Chewonarin, 2022) was assayed as well, in both basal and hydrogen peroxide-induced oxidative stress conditions. The hydrogen peroxide stimulus was chosen for its capability to increase the gene expression of the abovementioned factors, in colon cancer cells (Chiavaroli et al., 2023; Recinella et al., 2022). Particularly, the reduction of the gene expression of TNFα, HIF1α, and VEGFA (Fig. 9**A-C**) indicates the capability of the extract in contrasting cancer cell proliferation and angiogenesis (Kim et al., 2015; Wei et al., 2023; Zhang & Luo, 2018). The inhibition of TNFα gene expression is also consistent with the anti-inflammatory effects demonstrated by garlic extracts in the colon (Recinella et al., 2022). A new field of research is also considering the involvement of TRPM8 in colon carcinogenesis (Borrelli et al., 2014; Liu, Li, & Xu, 2022). Additionally, recent findings of ours suggested a relationship between cytotoxic effect and reduced TRPM8 gene expression,

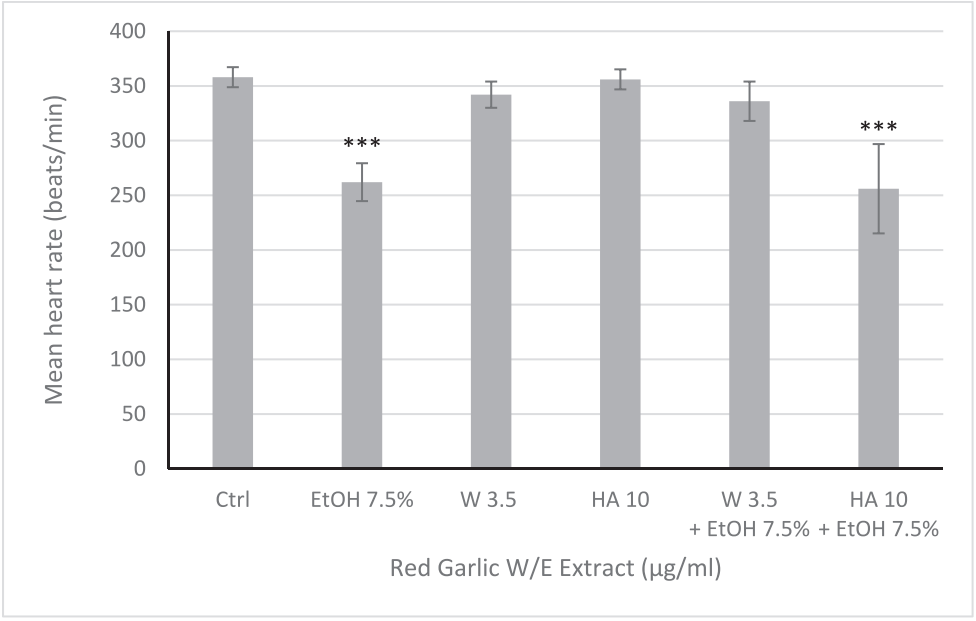

Fig. 7. Null effect of the hydroalcoholic (W/E) extract of aerial bulbils from "Sulmona Red Garlic" on the heart rate of *Daphnia magna* (*Daphnia magna* heartbeat rate test). ANOVA, $P < 0.0001$, ***$P < 0.001$ vs. Ctrl (Control group).

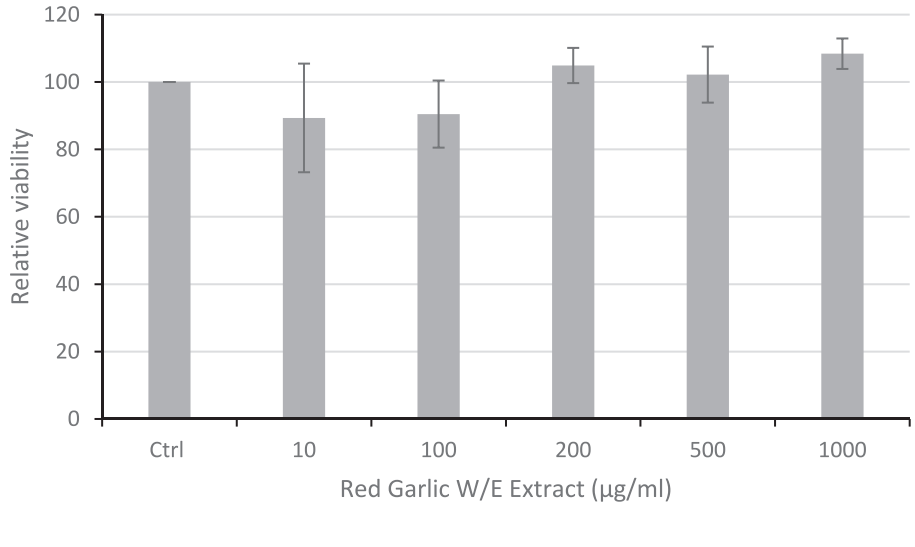

(A)

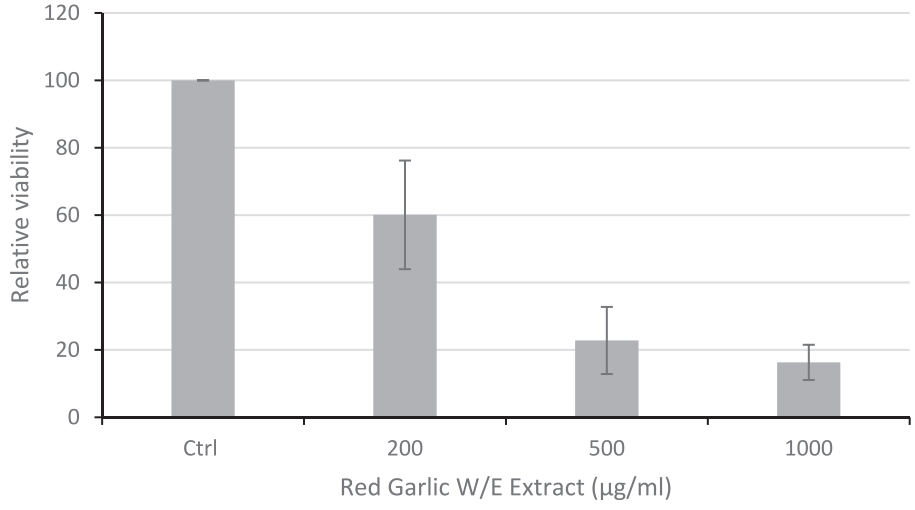

(B)

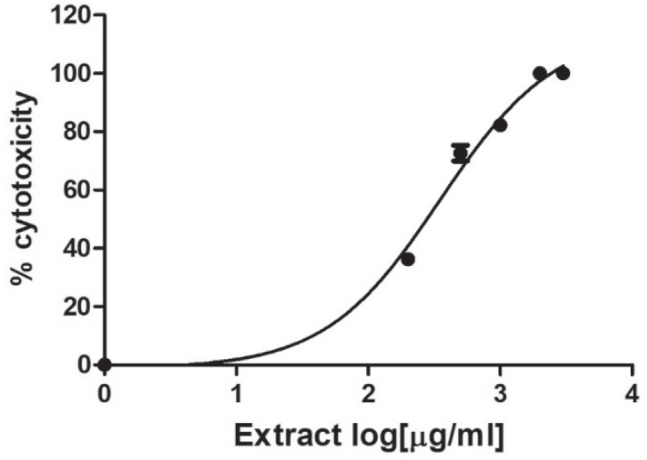

(C)

Fig. 8. Effects of the hydroalcoholic (W/E) extract of aerial bulbils from "Sulmona Red Garlic" on the C2C12 and HCT116 (B) cell line viability. The extract exerted a cytotoxic effect only on the human colon cancer HCT116 cell line (C: IC_{50}: 352.07 μg/mL). ANOVA, $P < 0.0001$; ***$P < 0.001$ vs. Ctrl (Control group).

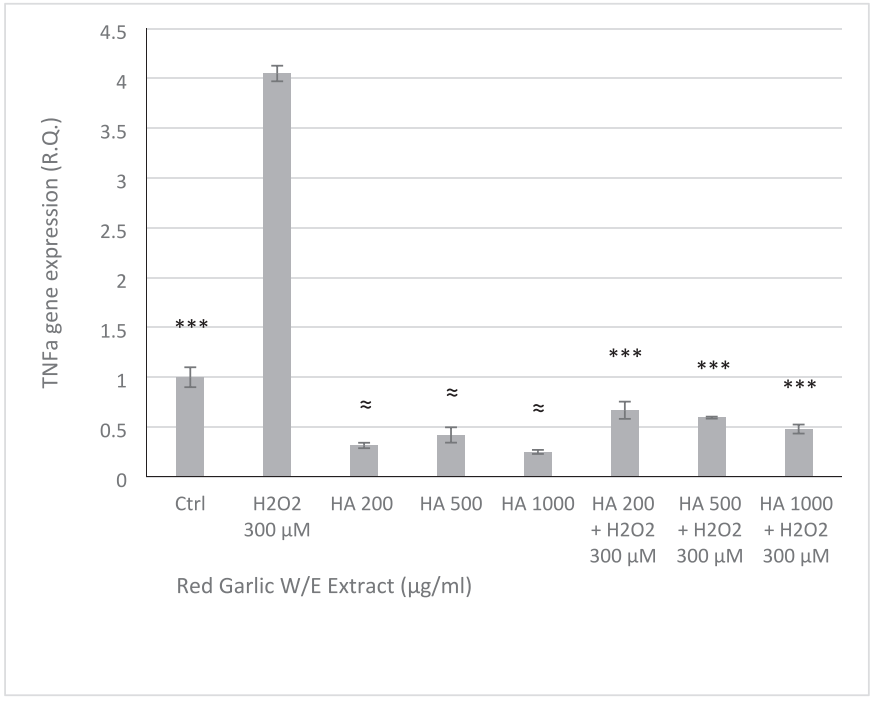

(A)

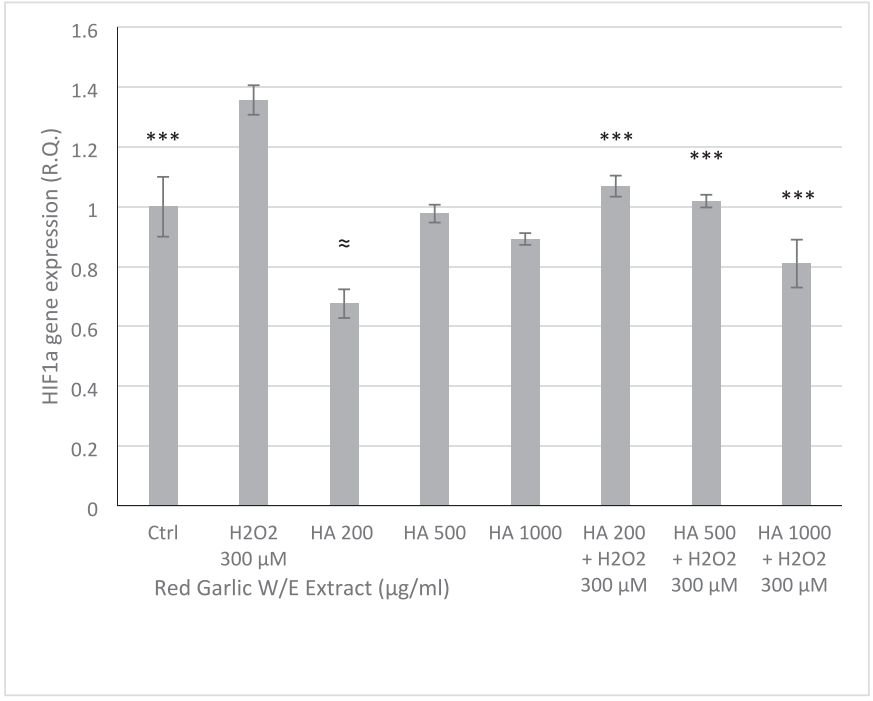

(B)

Fig. 9. Inhibitory effect induced by the hydroalcoholic extract of aerial bulbils from "Sulmona Red Garlic" on basal and hydrogen peroxide induced TNFα (A), HIF1α (B), VEGFA (C), and TRPM8 (C) gene expression, in HCT116 cells. A: ANOVA, $P < 0.0001$; ***$P < 0.001$ vs. hydrogen peroxide (H.P.); ≈$P < 0.0001$ vs Ctrl (Control group). B: ANOVA, $P < 0.0001$; ***$P < 0.001$ vs. hydrogen peroxide (H.P.); ≈$P < 0.0001$ vs Ctrl (Control group). C: ANOVA, $P < 0.0001$; ***$P < 0.001$ vs. hydrogen peroxide (H.P.); ≈$P < 0.0001$ vs Ctrl (Control group). D: ANOVA, $P < 0.0001$; ***$P < 0.001$ vs. hydrogen peroxide (H.P.); ≈$P < 0.0001$ vs Ctrl (Control group). (For interpretation of the references to colour in this figure legend, the reader is referred to the web version of this article.)

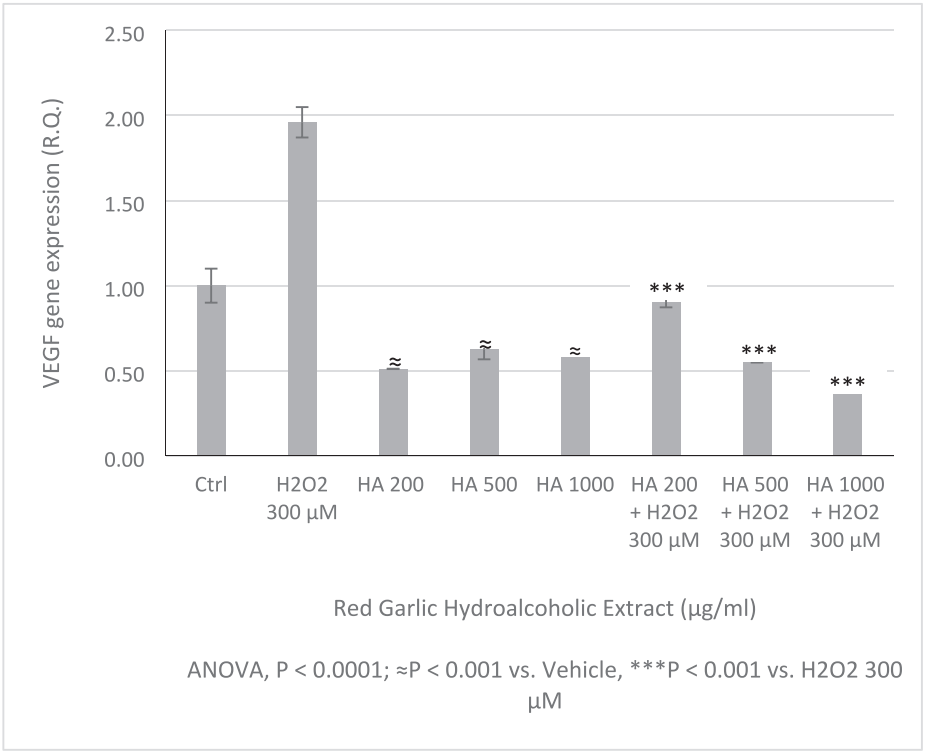

(C)

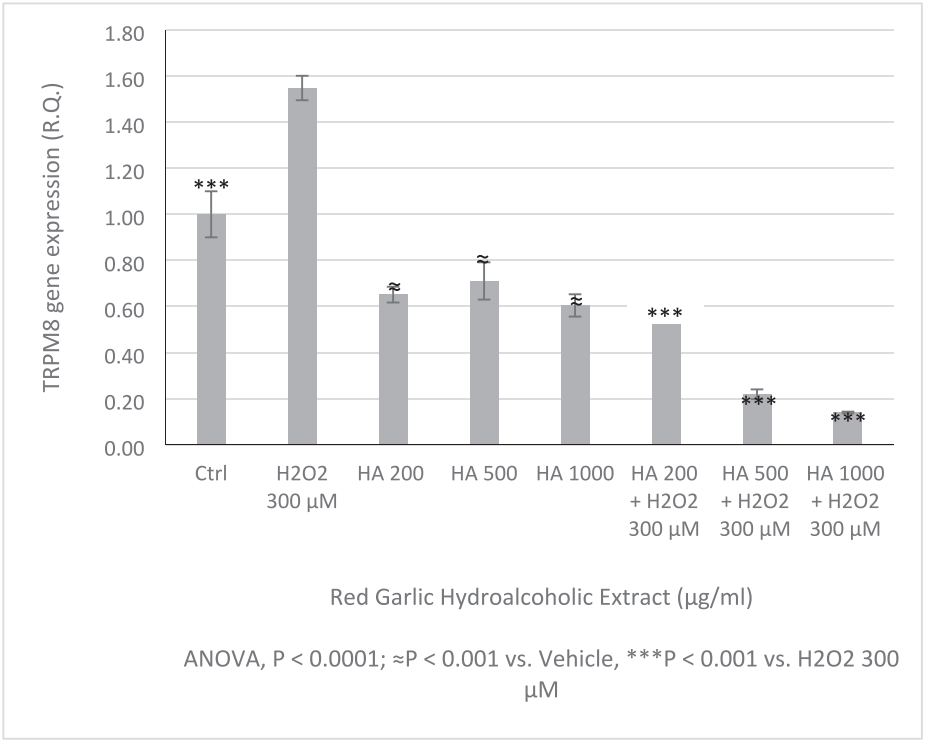

(D)

Fig. 9. (*continued*).

in colon cancer cells, in vitro (Chiavaroli et al., 2023; Recinella et al., 2022). In the present study, the hydroalcoholic extract of aerial bulbils form "Sulmona Red Garlic" reduced the gene expression of TRPM8 (Fig. 9**D**); thus, pointing to the inhibition of TRPM8 gene expression as one of the possible mechanisms underlying the extract-induced cytotoxic effect against HCT116 cells. The gene expression inhibition of all tested proteins could be related, albeit partially, to the extract's content in phenolic compounds, among which catechin demonstrated a direct

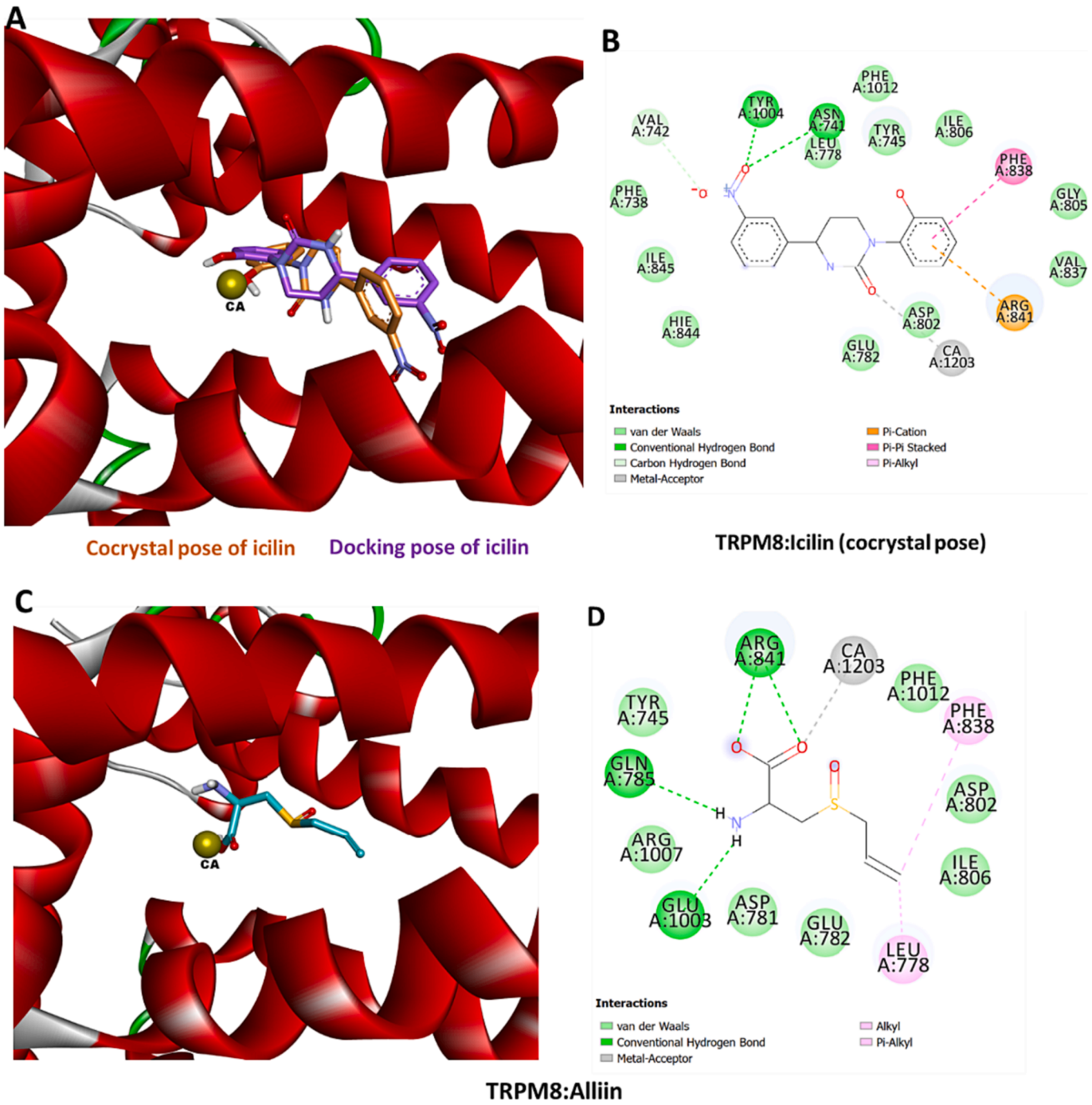

Fig. 10. (A) Validation of docking method: superimposition of the cocrystal pose of icilin in the cryo-EM structure of the TRPM8 ion channel complexed with icilin (PDB ID: 6NR3) with the docking pose (B) interaction between icilin and TRPM8. (C) Binding pose of alliin in the binding pocket of TRPM8, and (D) interaction between alliin and TRPM8.

inhibitory effect on TRPM8 gene expression (Recinella et al., 2022).

3.5. *In silico studies*

Bioinformatics predictions conducted on the platform STITCH also suggested that alliin and allicin could play a pivotal role in mediating extract-induced cytotoxic effect, as demonstrated by their putative interactions with HIF1 signaling pathway (pathway ID 04066), TNF signaling pathway (pathway ID 04668), VEGF signaling pathway (pathway ID 04370), and TRP channels pathway (pathway ID 04750).

Regarding the TRPM8, a docking approach was also conducted to calculate the putative affinities of both alliin and allicin towards this endovanilloid receptor. To validate the binding-mode predictive ability of AutoDock 4.2.6, the cocrystal ligand icilin was redocked into its cognate protein TRPM8. The cocrystal and docking poses of icilin were superimposed in the binding pocket of TRPM8 with the root-mean-square displacement (RMSD) value of 1.74 Å (Fig. 10**A**). An RMSD value of < 2.00 Å suggests that a docking pose is well predicted (Uba and Yelekçi, 2019). In the cocrystal pose, icilin bound to the TRPM8 via variety of interactions, including metal-acceptor interaction between the Ca^{2+} ion and oxo substituent; H-bonds with Asn71 and Tyr1004. Other interactions comprise π-cation, π-π stacked, and multiple van der

Waals interactions all over the binding pocket (Fig. 10**B**). Similarly, allium was completely buried in the binding channel of TRPM8 (Fig. 10**C**). Alliin engaged Ca^{2+} ion in metal-acceptor interaction via its carbonyl oxygen, formed H-bonds with Gln785, Arg841, and Glu1003; hydrophobic interactions with Leu778 and Phe838; and multiple van der Waals interactions with the residues lining the TRPM8 pocket (Fig. 10**D**). These interactions yielded a docking binding energy score of −6.84 kcal/mol, which is very much comparable with the docking score of the cocrystal ligand, icilin (-6.77 kcal/mol). Thus, alliin likely exerts its activity by interacting with TRPM8. An acceptable affinity for the receptor was calculated for only alliin (9.83 μM), and this is consistent with possible direct interactions between the compound and the receptor. Whilst allicin showed a putative affinity > 100 μM (data not shown); thus, ruling out any direct interaction between allicin and TRPM8. By contrast, allicin demonstrated to activate endovanilloid channels TRPV1 and TRPA1, thus indicating analgesic properties of this compounds (Hernández-Cruz et al., 2022; Xiao et al., 2021).

The ethanolic extract (EtOH:H2O 1:1 v/v) of the red garlic aerial bulbils, submitted to biological evaluation, was also analysed by NMR spectroscopy to assess the presence of alliin and other organosulphur compounds. The results clearly showed that the metabolomic profile was consistent with that of the hydroalcoholic phase of the Bligh-Dyer extract, which included OSCs such as allicin, methiin, alliin and cycloalliin, to which the activity on HCT116 cells and the affinity towards TRPM8 receptor are attributable.

4. Conclusion

In the present study, the composition and biological activity of the hydroalcoholic extract from the aerial bulbils of the *A. sativum* ecotype "Sulmona Red Garlic" was investigated. The extract was analyzed using a multi-methodological approach. The untargeted NMR spectroscopy provided valuable insights regarding several classes of metabolites in the hydroalcoholic extract of red garlic aerial bulbils. This includes organosulphur compounds such as alliin, allicin, methiin, and cycloalliin, all of which were quantified except for alliin. Targeted analysis allowed to identify and quantify secondary metabolites belonging to polyphenols. Aerial bulbils showed a chemical profile rich in healthy compounds to which the biological effect of the extract is attributable, confirming their promising phytotherapeutic use. The extract was effective in inducing a cytotoxic effect against human colon cancer HCT116 cells, in the concentration range 200–1000 μg/mL. In parallel, the gene expression of TNFα, HIF1α, VEGFA, and TRPM8 was reduced. Both sulphur and phenolic compounds could be responsible, albeit partially, of such effects. Intriguingly, the extract was well-tolerated by the non-tumoral C2C12 cell line, in the same concentration-range; thus, further suggesting the biocompatibility of the tested extract.

Concluding, the present study demonstrated the potential application of a plant material, the aerial bulbils, that is currently considered as waste material. However, the careful and manual work selection of harvested garlic plants makes the aerial bulbils an innovative and high-quality by-product, with promising health-promoting applications, as demonstrated by the metabolomics and biological data. Indeed, aerial bulbils could be considered as secondary material on which to base the development of innovative products such as food supplements with protective effects in the colon. This could lead to an overall improvement of the whole "Sulmona Red Garlic" productive chain.

Funding

This work was supported by the following grants: National Grant "Progetti di Rilevante Interesse Nazionale" (PRIN) 2017 from MIUR, Grant/Award Number: 2017XC73BW; National Recovery and Resilience Plan (NRRP, Mission 4 Component 2 Investment 1.3 – Call for tender No. 341 of 15 March 2022 of Italian Ministry of University and Research funded by the European Union – NextGenerationEU (Project code PE00000003, Concession Decree No. 1550 of 11 October 2022 adopted by the Italian Ministry of University and Research, CUP D93C22000890001, Project title "ON Foods – Research and innovation network on food and nutrition Sustainability, Safety and Security – Working ON Foods").]

Declaration of Competing Interest

The authors declare that they have no known competing financial interests or personal relationships that could have appeared to influence the work reported in this paper.

Data availability

Data will be made available on request.

Acknowledgements

The present study is also part of the third mission activities of the botanical garden "Giardino dei Semplici" of "G. d'Annunzio" University. The authors would like to thank Vittorio D'Alessandro ("Aglio D'Alessandro" company, Pratola Peligna, L'Aquila, Italy) for providing the plant material free of charge.

Appendix A. Supplementary data

Supplementary data to this article can be found online at https://doi.org/10.1016/j.foodres.2023.113654.

References

Acquaviva, A., Di Simone, S. C., Canini, A., Braglia, R., Di Marco, G., Campana, C., et al. (2022). Phytochemical and biological investigations on the pollen from industrial hemp male inflorescences. *Food Research International, 161*, Article 111883.

Albayati, S., Uba, A. I., & Yelekçi, K. (2022). Potential inhibitors of methionine aminopeptidase type II identified via structure-based pharmacophore modeling. *Molecular Diversity*, 1–12.

Ansary, J., Forbes-Hernández, T. Y., Gil, E., Cianciosi, D., Zhang, J., Elexpuru-Zabaleta, M., et al. (2020). Potential health benefit of garlic based on human intervention studies: A brief overview. *Antioxidants, 9*(7), 619.

Biancolillo, A., Marini, F., & D'Archivio, A. A. (2020). Geographical discrimination of red garlic (Allium sativum L.) using fast and non-invasive Attenuated Total Reflectance-Fourier Transformed Infrared (ATR-FTIR) spectroscopy combined with chemometrics. *Journal of Food Composition and Analysis, 86*, Article 103351. https://doi.org/10.1016/j.jfca.2019.103351

Bligh, E. G., & Dyer, W. J. (1959). A rapid method of total lipid extraction and purification (Can. *J. Biochem. Physiol., 37*, 911–917.

Block, E. (1992). The Organosulfur Chemistry of the Genus Allium – Implications for the Organic Chemistry of Sulfur. *Angewandte Chemie International Edition in English, 31* (9), 1135–1178. https://doi.org/10.1002/anie.199211351

Borlinghaus, J., Albrecht, F., Gruhlke, M. C. H., Nwachukwu, I. D., & Slusarenko, A. J. (2014). Allicin: Chemistry and biological properties. *Molecules (Basel, Switzerland), 19*(8), 12591–12618. https://doi.org/10.3390/molecules190812591

Borrelli, F., Pagano, E., Romano, B., Panzera, S., Maiello, F., Coppola, D., et al. (2014). Colon carcinogenesis is inhibited by the TRPM8 antagonist cannabigerol, a Cannabis-derived non-psychotropic cannabinoid. *Carcinogenesis, 35*(12), 2787–2797.

Brunetti, L., Menghini, L., Orlando, G., Recinella, L., Leone, S., Epifano, F., et al. (2009). Antioxidant effects of garlic in young and aged rat brain in vitro. *Journal of medicinal food, 12*(5), 1166–1169.

X. Chen C. Xu S. Hong X. Xia Y. Cao J. McDermott et al. Immune cell types and secreted factors contributing to inflammation-to-cancer transition and immune therapy response Cell Reports 26 7 2019 1965–1977. e1964.

Chiavaroli, A., Balaha, M., Acquaviva, A., Ferrante, C., Cataldi, A., Menghini, L., et al. (2021). Phenolic characterization and neuroprotective properties of grape pomace extracts. *Molecules, 26*(20), 6216.

A. Chiavaroli M.L. Libero S.C. Di Simone A. Acquaviva R. Nilofar L., Leone, S., Brunetti, L., Cicia, D., & Izzo, A. A. Adding New Scientific Evidences on the Pharmaceutical Properties of *Pelargonium quercetorum* Agnew Extracts by Using In Vitro and In Silico Approaches Plants 12 5 2023 1132.

Dehghanian, Z., Habibi, K., Dehghanian, M., Aliyar, S., Lajayer, B. A., Astatkie, T., et al. (2022). Reinforcing the bulwark: Unravelling the efficient applications of plant phenolics and tannins against environmental stresses. *Heliyon, e09094*.

Ferioli, F., Giambanelli, E., D'Alessandro, V., & D'Antuono, L. F. (2020). Comparison of two extraction methods (high pressure extraction vs. Maceration) for the total and relative amount of hydrophilic and lipophilic organosulfur compounds in garlic cloves and stems. An application to the Italian ecotype "Aglio Rosso di Sulmona". *Food Chemistry, 312*, Article 126086. https://doi.org/10.1016/j.foodchem.2019.126086. Sulmona Red Garlic.

Ferrante, C., Recinella, L., Ronci, M., Menghini, L., Brunetti, L., Chiavaroli, A., et al. (2019). Multiple pharmacognostic characterization on hemp commercial cultivars: Focus on inflorescence water extract activity. *Food and Chemical Toxicology, 125*, 452–461.

Gomez, L., Vercambre, G., & Jordan, M.-O. (2020). Spatial-temporal management of nitrogen and carbon on the peach tree (Prunus persicae L. Batsch.). *Scientia Horticulturae, 273*, Article 109613. https://doi.org/10.1016/j.scienta.2020.109613

Hakamata, W., Koyama, R., Tanida, M., Haga, T., Hirano, T., Akao, M., et al. (2015). A Simple Synthesis of Alliin and allo-Alliin: X-ray Diffraction Analysis and Determination of Their Absolute Configurations. *Journal of Agricultural and Food Chemistry, 63*(50), 10778–10784. https://doi.org/10.1021/acs.jafc.5b05501

Hernández-Cruz, E.Y., Silva-Islas, C.A., Maldonado, P.D., Pedraza-Chaverri, J., Carballo-Villalobos, A.I. (2022). Antinociceptive effect of garlic, garlic preparations and derivative compounds. *European Journal of Pain, 26*(5), 947–964. doi: 10.1002/ejp.1935. Epub 2022 Mar 22. PMID: 35263014. https://www.fondazioneslowfood.com/en/ark-of-taste-slow-food/sulmona-red-garlic.

Ingallina, C., Di Matteo, G., Spano, M., Acciaro, E., Campiglia, E., Mannina, L., et al. (2023). Byproducts of Globe Artichoke and Cauliflower Production as a New Source of Bioactive Compounds in the Green Economy Perspective: An NMR Study. *Molecules, 28*(3), 1363.

Jones, M. G., Hughes, J., Tregova, A., Milne, J., Tomsett, A. B., & Collin, H. A. (2004). Biosynthesis of the flavour precursors of onion and garlic. *Journal of Experimental Botany, 55*(404), 1903–1918. https://doi.org/10.1093/jxb/erh138

Kajimura, Y., Sugiura, T., Suenaga, K., Itakura, Y., & Etoh, T. (2000). A new garlic growing system from bulbils through transplanting. *The Journal of Horticultural Science and Biotechnology, 75*(2), 176–180. https://doi.org/10.1080/14620316.2000.11511219

Kasprzak-Drozd, K., Oniszczuk, T., Kowalska, I., Mołdoch, J., Combrzyński, M., Gancarz, M., et al. (2022). Effect of the Production Parameters and In Vitro Digestion on the Content of Polyphenolic Compounds, Phenolic Acids, and Antiradical Properties of Innovative Snacks Enriched with Wild Garlic (Allium ursinum L.) Leaves. *International Journal of Molecular Sciences, 23*(22). https://doi.org/10.3390/ijms232214458

Keller, E. R., & Senula, A. (2013). Micropropagation and cryopreservation of garlic (Allium sativum L.). *Methods in Molecular Biology, 11013*, 353–368. https://doi.org/10.1007/978-1-62703-074-8_28

Kim, D. H., Sung, B., Kang, Y. J., Hwang, S. Y., Kim, M. J., Yoon, J.-H., et al. (2015). Sulforaphane inhibits hypoxia-induced HIF-1α and VEGF expression and migration of human colon cancer cells. *International journal of oncology, 47*(6), 2226–2232.

Kopeć, A., Skoczylas, J., Jędrszczyk, E., Francik, R., Bystrowska, B., & Zawistowski, J. (2020). Chemical composition and concentration of bioactive compounds in garlic cultivated from air bulbils. *Agriculture, 10*(2), 40.

Lasalvia, A., Cairone, F., Cesa, S., Maccelli, A., Crestoni, M. E., Menghini, L., et al. (2022). Characterization and Valorization of 'Sulmona Red Garlic'Peels and Small Bulbs. *Antioxidants, 11*(11), 2088.

Liang, T., Wei, F., Lu, Y., Kodani, Y., Nakada, M., Miyakawa, T., et al. (2015). Comprehensive NMR Analysis of Compositional Changes of Black Garlic during Thermal Processing. *Journal of Agricultural and Food Chemistry, 63*(2), 683–691. https://doi.org/10.1021/jf504836d

Liu, L., & Yeh, Y. Y. (2000). Inhibition of cholesterol biosynthesis by organosulfur compounds derived from garlic. *Lipids, 35*(2), 197–203. https://doi.org/10.1007/BF02664770

Liu, J. J., Li, L. Z., & Xu, P. (2022). Upregulation of TRPM8 can promote the colon cancer liver metastasis through mediating Akt/GSK-3 signal pathway. *Biotechnology and Applied Biochemistry, 69*(1), 230–239.

Livak, K. J., & Schmittgen, T. D. (2001). Analysis of relative gene expression data using real-time quantitative PCR and the 2− ΔΔCT method. *Methods, 25*(4), 402–408.

Llorent-Martínez, E. J., Ruiz-Medina, A., Zengin, G., Ak, G., Jugreet, S., Mahomoodally, M. F., Emre, G., Orlando, G., Libero, M. L., & Acquaviva, A. (2022). New Biological and Chemical Evidences of Two Lamiaceae Species (*Thymbra capitata* and *Thymus sipyleus* subsp. rosulans): *In Vitro*, *In Silico* and Ex Vivo Approaches. *Molecules, 27*(24), 9029.

Mannina, L., Sobolev, A. P., & Capitani, D. (2012). Applications of NMR metabolomics to the study of foodstuffs: Truffle, kiwifruit, lettuce, and sea bass. *Electrophoresis, 33*(15), 2290–2313. https://doi.org/10.1002/elps.201100668

Mannina, L., Sobolev, A. P., & Viel, S. (2012). Liquid state 1H high field NMR in food analysis. *Progress in Nuclear Magnetic Resonance Spectroscopy, 66*, 1–39. https://doi.org/10.1016/j.pnmrs.2012.02.001

Martínez-Rosell, G., Giorgino, T., & De Fabritiis, G. (2017). PlayMolecule ProteinPrepare: A web application for protein preparation for molecular dynamics simulations. *Journal of chemical information and modeling, 57*(7), 1511–1516.

D. Mathew Z. Ahmed N. Singh Formulation of Flowering Index, Morphological Relationships, and Yield Prediction System in True Garlic Aerial Seed Bulbil Production HortScience HortSci 40 7 2005 2036 2039 https://doi.org/10.21273/HORTSCI.40.7.2036.

Menghini, L., Ferrante, C., Leporini, L., Recinella, L., Chiavaroli, A., Leone, S., et al. (2016). An hydroalcoholic chamomile extract modulates inflammatory and immune response in HT29 cells and isolated rat colon. *Phytotherapy research, 30*(9), 1513–1518.

Menghini, L., Leporini, L., Vecchiotti, G., Locatelli, M., Carradori, S., Ferrante, C., et al. (2018). *Crocus sativus* L. stigmas and byproducts: Qualitative fingerprint, antioxidant potentials and enzyme inhibitory activities. *Food Research International, 109*, 91–98.

Nantz, M. P., Rowe, C. A., Muller, C. E., Creasy, R. A., Stanilka, J. M., & Percival, S. S. (2012). Supplementation with aged garlic extract improves both NK and γδ-T cell function and reduces the severity of cold and flu symptoms: A randomized, double-blind, placebo-controlled nutrition intervention. *Clinical Nutrition (Edinburgh, Scotland), 31*(3), 337–344. https://doi.org/10.1016/j.clnu.2011.11.019

Orlando, G., Chiavaroli, A., Adorisio, S., Delfino, D. V., Brunetti, L., Recinella, L., et al. (2021). Unravelling the phytochemical composition and the pharmacological properties of an optimized extract from the fruit from *Prunus mahaleb* L.: From traditional liqueur market to the pharmacy shelf. *Molecules, 26*(15), 4422.

Panyathep, A., Punturee, K., & Chewonarin, T. (2022). Gamma-Oryzanol-Rich Fraction from Purple Rice Extract Attenuates Lipopolysaccharide-Stimulated Inflammatory Responses, Migration and VEGFA Production in SW480 Cells via Modulation of TLR4 and NF-κB Pathways. *Nutrition and Cancer, 74*(6), 2254–2264.

Putnik, P., Gabrić, D., Roohinejad, S., Barba, F. J., Granato, D., Mallikarjunan, K., et al. (2019). An overview of organosulfur compounds from *Allium* spp.: From processing and preservation to evaluation of their bioavailability, antimicrobial, and anti-inflammatory properties. *Food Chemistry, 276*, 680–691. https://doi.org/10.1016/j.foodchem.2018.10.068

Recinella, L., Chiavaroli, A., Masciulli, F., Fraschetti, C., Filippi, A., Cesa, S., et al. (2021). Protective effects induced by a hydroalcoholic *Allium sativum* extract in isolated mouse heart. *Nutrients, 13*(7). https://doi.org/10.3390/nu13072332

Recinella, L., Chiavaroli, A., Veschi, S., Cama, A., Acquaviva, A., Libero, M. L., et al. (2022). A grape (Vitis vinifera L.) pomace water extract modulates inflammatory and immune response in SW-480 cells and isolated mouse colon. *Phytotherapy research, 36*(12), 4620–4630.

Recinella, L., Gorica, E., Chiavaroli, A., Fraschetti, C., Filippi, A., Cesa, S., et al. (2022). Anti-Inflammatory and Antioxidant Effects Induced by *Allium sativum* L. *Extracts on an Ex Vivo Experimental Model of Ulcerative Colitis. Foods, 11*(22), 3559.

Ritota, M., Casciani, L., Han, B.-Z., Cozzolino, S., Leita, L., Sequi, P., et al. (2012). Traceability of Italian garlic (Allium sativum L.) by means of HRMAS-NMR spectroscopy and multivariate data analysis. *Food chemistry, 135*(2), 684–693.

Rose, P., Whiteman, M., Moore, P. K., & Zhu, Y. Z. (2005). Bioactive S-alk(en)yl cysteine sulfoxide metabolites in the genus Allium: The chemistry of potential therapeutic agents. *Natural Product Reports, 22*(3), 351–368. https://doi.org/10.1039/b417639c

Saud, S. M., Li, W., Gray, Z., Matter, M. S., Colburn, N. H., Young, M. R., et al. (2016). Diallyl disulfide (DADS), a constituent of garlic, inactivates NF-κB and prevents colitis-induced colorectal cancer by inhibiting GSK-3β. *Cancer Prevention Research, 9*(7), 607–615.

Saviano, G., Paris, D., Melck, D., Fantasma, F., Motta, A., & Iorizzi, M. (2019). Metabolite variation in three edible Italian *Allium cepa* L. by NMR-based metabolomics: A comparative study in fresh and stored bulbs. *Metabolomics, 15*(8), 105. https://doi.org/10.1007/s11306-019-1566-6

Shirin, H., Pinto, J. T., Kawabata, Y., Soh, J. W., Delohery, T., Moss, S. F., et al. (2001). Antiproliferative effects of S-allylmercaptocysteine on colon cancer cells when tested alone or in combination with sulindac sulfide. *Cancer Research, 61*(2), 725–731.

Šnirc, M., Lidiková, J., Čeryová, N., Pintér, E., Ivanišová, E., Musilová, J., et al. (2023). Mineral and phytochemical profiles of selected garlic (Allium sativum L.) cultivars. *South African Journal of Botany, 158*, 319–325. https://doi.org/10.1016/j.sajb.2023.05.024

Spano, M., Di Matteo, G., Ingallina, C., Botta, B., Quaglio, D., Ghirga, F., Balducci, S., Cammarone, S., Campiglia, E., Giusti, A. M., Vinci, G., Rapa, M., Ciano, S., Mannina, L., & Sobolev, A. P. (2021). A Multimethodological Characterization of *Cannabis sativa* L. Inflorescences from Seven Dioecious Cultivars Grown in Italy: The Effect of Different Harvesting Stages. *Molecules, 26* (10). 10.3390/molecules26102912.

Spano, M., Di Matteo, G., Fernandez Retamozo, C. A., Lasalvia, A., Ruggeri, M., Sandri, G., et al. (2023). A Multimethodological Approach for the Chemical Characterization of Edible Insects: The Case Study of *Acheta domesticus*. *Foods, 12*, 2331. https://doi.org/10.3390/foods12122331

Tanrıkulu, Y., Şen Tanrıkulu, C., Kılınç, F., Can, M., & Köktürk, F. (2020). Effects of garlic oil (Allium sativum) on acetic acid-induced colitis in rats: Garlic oil and experimental colitis. *Turk. J. Trauma Emerg. Surg, 26*, 503–508.

Vezza, T., Algieri, F., Garrido-Mesa, J., Utrilla, M. P., Rodríguez-Cabezas, M. E., Banos, A., et al. (2019). The Immunomodulatory Properties of Propyl-Propane Thiosulfonate Contribute to its Intestinal Anti-Inflammatory Effect in Experimental Colitis. *Molecular nutrition & food research, 63*(5), 1800653.

Villegas-Navarro, A., Rosas-L, E., & Reyes, J. L. (2003). The heart of Daphnia magna: Effects of four cardioactive drugs. *Comparative Biochemistry and Physiology Part C: Toxicology & Pharmacology, 136*(2), 127–134.

Wei, W., Wang, J., Huang, P., Gou, S., Yu, D., & Zong, L. (2023). Tumor necrosis factor-α induces proliferation and reduces apoptosis of colorectal cancer cells through STAT3 activation. *Immunogenetics, 75*(2), 161–169.

Xiao, S., Song, P., Bu, F., Pang, G., Zhou, A., Zhang, Y., et al. (2021). The investigation of detection and sensing mechanism of spicy substance based on human TRPV1 channel protein-cell membrane biosensor. *Biosensors and Bioelectronics, 172*, Article 112779. https://doi.org/10.1016/j.bios.2020.112779

Xu, C., Mathews, A. E., Rodrigues, C., Eudy, B. J., Rowe, C. A., O'Donoughue, A., et al. (2018). Aged garlic extract supplementation modifies inflammation and immunity of adults with obesity: A randomized, double-blind, placebo-controlled clinical trial. *Clinical Nutrition ESPEN, 24*, 148–155. https://doi.org/10.1016/j.clnesp.2017.11.010

Yan, J.-Y., Tian, F.-M., Hu, W.-N., Zhang, J.-H., Cai, H.-F., & Li, N. (2013). Apoptosis of human gastric cancer cells line SGC 7901 induced by garlic-derived compound S-allylmercaptocysteine (SAMC). *European Review for Medical and Pharmacological Sciences, 17*(6), 745–751.

Yang, P., Xu, L., Xu, H., Tang, Y., He, G., Cao, Y., et al. (2017). Histological and Transcriptomic Analysis during Bulbil Formation in *Lilium lancifolium*. *Frontiers in Plant Science, 8*, 1508. https://doi.org/10.3389/fpls.2017.01508

Zhang, X., & Luo, H. (2018). Effects of thalidomide on growth and VEGF-A expression in SW480 colon cancer cells. *Oncology Letters, 15*(3), 3313–3320.